Structural Engineering and Mechanics, *Vol. 68, No. 1 (2018) 131-157*
DOI: https://doi.org/10.12989/sem.2018.68.1.131

Vibration characteristics of advanced nanoplates in humid-thermal environment incorporating surface elasticity effects via differential quadrature method

Farzad Ebrahimi* and Ebrahim Heidari

Department of Mechanical Engineering, Faculty of Engineering, Imam Khomeini International University, Qazvin, Iran

(Received May 5, 2018, Revised June 22, 2018, Accepted June 25, 2018)

Abstract. In this study, Eringen nonlocal elasticity theory in conjunction with surface elasticity theory is employed to study nonlinear free vibration behavior of FG nano-plate lying on elastic foundation, on the base of Reddy's plate theory. The material distribution is assumed as a power-law function and effective material properties are modeled using Mori-Tanaka homogenization scheme. Hamilton's principle is implemented to derive the governing equations which solved using DQ method. Finally, the effects of different factors on natural frequencies of the nano-plate under hygrothermal situation and various boundary conditions are studied.

Keywords: nanomechanics; rectangular plate; hygro-thermo-mechanical; surface effect; generalized differential quadrature method; high shear deformation plate theory; thermal loading; elastic medium; nonlocal

1. Introduction

Nano electro mechanical systems (NEMS), are one of targets which today's human being try to develop his science in, because of its high performance; in fact, this efficiency emanates from the superior mechanical, chemical and electronic properties of elements used in NEMS; however, experimental studies in this field have been faced with many difficulties to conduct and then theoretical studies play a prominent role in advancing this knowledge (Ansari *et al.* 2015); meanwhile, as powerful tools, numerical methods have been often used to solve related complicated equations (Chen and Li 2013, Ebrahimi and Hosseini 2016a).

To Enhanced material properties of any nanostructure, we can compose different materials gradually in one another to gain a nanostructure called nano-FGM structure. Nano-plates are one of nanostructures which are used a lot in NEMS; also, they are widely used as resonators and sensors that may tolerate very high frequencies up to 1 gigahertz (Panyatong *et al*. 2015); therefore, it is important to study the vibrational behavior of nano-plates. There are a lot of research that study the vibrational behavior of nano-plates and FG nano-plates; Malekzadeh and Shojaee (2015), studied the influences of nonlocal and surface effects on the vibration of nano-plates by the use of first-order shear deformation theory. They showed that surface energy increases the natural frequencies and small-scale effect reduces them. Using first shear deformation theory, Ansari and Gholami (2016), analyzed the effect of surface stresses on the large amplitude periodic forced vibration of rectangular nano-plates and concluded that in terms of nonlinear frequency, the effects of surface on aluminum is more considerable than silicon nano-plates. On the basis of the Kirchhoff's plate model, Karimi *et al.* (2017) incorporate nonlocal continuum and surface effects to investigate the buckling and vibration of nano-plates. It is inferred that the effects of surface on the buckling and vibration of nano-plates to be increased with enhancing nano-plate aspect ratio and decreasing its thickness. With an exact analytical solution, Salehipour *et al.* (2015) studied the free vibration of functionally graded micro/nano-plate using nonlocal elasticity and three-dimensional plate theory. Nami and Janghorban (2015) developed an analytical solution to analyze the free vibration analysis of functionally graded rectangular nano-plates based on second order shear deformation and nonlocal elasticity theory; they showed that increasing power law index and length to thickness ratio will decrease the natural frequencies. Choosing Kirchhoff, Mindlin and third order shear deformation theories as displacement filed, Ghassabi *et al.* (2017), compared the effects of factors such as nonlocal parameter and power –law index on vibration behavior of functionally graded rectangular nano-plate for simply-supported and cantilever nano-plates. Belkorissat *et al.* (2015) presented a new nonlocal refined plate theory to study free vibration behavior of FG nano-plates which is modeled by Mori-Tanaka homogenization scheme. Sobhy and Radwan (2017) investigated free vibration and buckling behavior of FG nanoplates with quasi-3D plate theory in thermal environment. Using linear methods and on the base of Kirchhoff's plate theory, Zare *et al.* (2015) studied the vibration response of rectangular FG nanoplates for different boundary conditions. Daneshmehr *et al.* (2015) used higher order shear deformation plate theory to investigate linear free vibration of FG nano-plate resting on elastic foundation. A study of biaxial buckling and free vibration behavior of FG

*Corresponding author, Professor
E-mail: febrahimy@eng.ikiu.ac.ir

ISSN: 1225-4568 (Print), 1598-6217 (Online)

nano-plates was presented by Hosseini and Jamalpoor (2017) in which the FG nano-plate was embedded in visco-Pasternak foundation; using Kirchhoff's plate theory they concluded that the effect of surface layer on damped natural frequency and buckling load is significantly dependent on the mode's degree. Thermal and moisture analysis in structures and nano -structures has been one of prominant subjects for many researchers (Ebrahimi and Hosseini 2016b, Ebrahimi and Barati 2018a, Ebrahimi and Salari 2015). Sobhy (2015) developed a comprehensive study on bending, free vibration, mechanical and thermal buckling of FG nano-plates resting on elastic foundation; in his research, the use of linear strain-displacement relations and refined shear deformation plate theory conduced to this result that nonlocal parameter has noticeable effect on the stiffness of the FG nano-plates. Panyatong *et al.* (2016) presented free vibration analysis of simply supported second order FG nano-plate embedded in an elastic medium based on nonlocal elasticity of Eringen; they assumed that the FG nano-plate is under an applied uniform thermal load and material properties are temperature dependent. By the use of linear assumption, Ebrahimi and Barati (2017a) tried to show the influence of physical fields such as moisture, temperature, electric voltage and magnetic fields on vibration and buckling responses of FG Refined nano-plates. In other research, Barati *et al.* (2016) employed refined plate theory of inverse cotangential type to investigate thermal buckling behavior of embedded nano FG plates and they found that nonlocal parameters, material composition and plate geometrical parameters influence the critical buckling temperature. Based on refined plate theory and Mori -Tanaka homogenization scheme, Nguyen *et al.* (2015) used IGA approach to analyze linear free vibration and buckling characteristics of FG simply and clamped supported boundary conditions. Thermal buckling and linear free vibration of FG nano-plates in conjunction with surface stresses studied by Ansari *et al.* (2015) using Kirchhoff's plate theory and linear temperature rise assumption. Finally, Barati and Shahverdi (2016, 2017) in their research, employed Refined plate theory to investigate thermal buckling and post-buckling and vibration characteristic of FG nano-plate for different boundary condition under hygro thermal situation; however, they used linear stress-strain relations for their research and neglected the surface stress effects in their study. Ebrahimi and Barati (2016g, h, I, j, k, l, m, n, o, p, q, r, s, t, u, v, 2017a, b) and Ebrahimi *et al.* (2017) explored thermal and hygro-thermal effects on nonlocal behavior of FG nanobeams and nanoplates.

In the present study, the nonlinear free vibration behavior of rectangular FG nano-plate is investigated. It is assumed that the FG nano-plate is embedded in elastic medium and FG material properties are modeled using Mori-Tanaka homogenization scheme. The governing equations are derived based on Eringen nonlocal elasticity in conjunction with Gurtin-Murdoch surface continuum theories. Knowing this consideration that distribution of FG material is according to power-law function and using Reddy's plate theory and GDQ method we study, the effect of nonlocal parameter, power-law distribution, geometrical parameters, Winkler and Pasternak parameters and surface parameters on natural frequencies of the nano-plate under hygrothermal

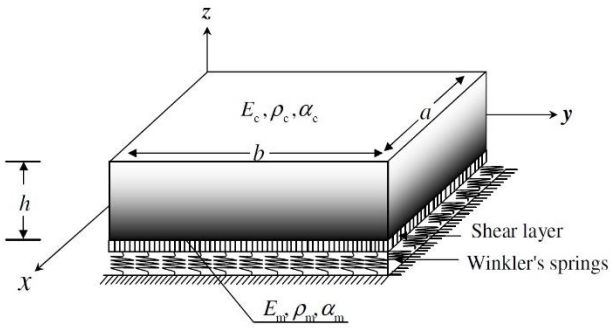

Fig. 1 Geometry of a rectangular FG nano-plate resting on Pasternak elastic foundation (Sobhy 2015)

situation and various boundary conditions. We also develop a comparison study to establish the validity of the provided solution. Considering surface effect, hygrothermal stress, elastic environment interaction and nonlinearity assumptions simultaneously is the main purpose of this paper.

2. Theoretical preliminaries

Consider a one directional FGM nao-plate of length a, width b and thickness h made from a mixture of ceramic (Silicon) and metal (Aluminum) resting on elastic foundation (Fig. 1); the upper surface (z=h/2) is ceramic-rich, the lower surface (z=-h/2) is metal rich and in between, the material composition has a gradual variation as a power law function

$$V_c = \left(\frac{1}{2} + \frac{z}{h}\right)^p \tag{1}$$

Where $0 \le V_c \le 1$ is ceramic volume fraction which is a function of elevation of each point in the nano FG plate; p is a volume fraction exponent.

If V_m is metal volume fraction, the relation between V_c and V_m at each elevation of nano-plate is

$$V_c + V_m = 1 \tag{2}$$

2.1 Effective material properties

According to Mori-Tanaka homogenization scheme (Qian *et al*. 2004, Shen 2016), the effective material properties can be found from these relations

$$\frac{K_f(z,T) - K_c(\hat{T})}{K_m(T) - K_c(T)} = \frac{V_m}{1 + (1 - V_m)(3(K_m(T) - K_c(T))/(3K_c(T) + 4G_c(T)))} \tag{3.1}$$

$$\frac{\dfrac{G_f(z,T) - G_c(T)}{G_m(T) - G_c(T)}}{\dfrac{V_m}{1 + (1 - V_m)((G_m(T) - G_c(T))/(G_c(T) + f_c))}} \tag{3.2}$$

$$\frac{\alpha_f(z,T) - \alpha_c(T)}{\alpha_m(T) - \alpha_c(T)} = \frac{\dfrac{1}{K_f(z,T)} - \dfrac{1}{K_c(T)}}{\dfrac{1}{K_m(T)} - \dfrac{1}{K_c(T)}} \tag{3.3}$$

$$\frac{\kappa_f(z,T)-\kappa_c(T)}{\kappa_m(T)-\kappa_c(T)} = \frac{V_m}{1+(1-V_m)((\kappa_m(T)-\kappa_c(T))/3\kappa_c(T))} \tag{3.4}$$

$$f_c = \frac{G_c(T)(9K_c(T)+8G_c(T))}{6(K_c(T)+2G_c(T))} \tag{3.5}$$

Where K, G, α and κ are respectively, the effective bulk modulus, the effective shear modulus, the effective thermal expansion coefficient and thermal conductivity; the subscripts "m", "c" and "f" denote metal, ceramic and effective property; in this relation all properties are temperature dependent (T denotes temperature).

About density it is inevitable to use the rule of mixture relation (Qian *et al*. 2004)

$$\rho_c V_c + \rho_m V_m = \rho_f \tag{4}$$

The temperature dependent material properties can be expressed as (Reddy 2011)

$$P = P_0(P_{-1}T^{-1} + 1 + P_1T + P_2T^2 + P_3T^3) \tag{5}$$

Where P is typical material property, P_0, P_{-1}, P_1, P_2 and P_3 are the coefficients of temperature; these coefficients can be obtained from reported data of exhibitions and tables (Aluminum Association 1984, Poirier and Geiger 2016) and using curve fitting methods (Ahn 2004); however, there is some explicit relations for some temperature dependent material properties like those reported in reference (Hull 1999); the present study utilizes Eq. (5) only for properties which there is no explicit relation for; Table 1 provide all of these relations for Al/Si nano-plates.

2.2 Kinematic relations

From Reddy's plate theory (Reddy 1984), a five-degrees-of-freedom relation for displacement field can be written as

$$u(x,y,z,t) = u_0(x,y,t) + z\varphi_x(x,y,t) - \frac{4z^3}{3h^2}\left(\varphi_x(x,y,t) + \frac{\partial w_0(x,y,t)}{\partial x}\right) \tag{6.1}$$

$$v(x,y,z,t) = v_0(x,y,t) + z\varphi_y(x,y,t) - \frac{4z^3}{3h^2}\left(\varphi_y(x,y,t) + \frac{\partial w_0(x,y,t)}{\partial y}\right) \tag{6.2}$$

$$w(x,y,z,t) = w_0(x,y,t) \tag{6.3}$$

Where (u,v,w) are displacements of the points of the nono-plate in (x,y,z) directions; (u_0,v_0,w_0) are displacements of each point at $(x,y,0)$ in (x,y,z) Cartesian coordinate system (the xy –plane of the Cartesian coordinate system is coincided with the geometric middle plane of the plate); φ_x and φ_y are bending rotations in y and x directions.

There is no doubt that Reddy's plate theory and other theories based on it, are the most complete which consider rotation, elongation (stretching effect) and curvature of perpendicular lines to the mid-surface (Reddy 2006); however there are many recent works which try using change of variable methods, lower the number of unknowns (Ebrahimi and Barati 2016a, Ebrahimi and Barati 2017b); Although these are promising methods, they don't consider elongation of transverse normal (Lee *et al*. 2015); by this way, these methods are more effective for linear assumptions. To remove this shortcoming, they necessarily introduce another variable to consider stretching effect (Lee *et al*. 2015); then the number of unknowns will again be five.

Table 1 Temperature dependent material properties

Property	Material	P_{-1}	P_0	P_1	P_2	P_3
$E(Gpa)$	Al[12] $0 \le T(K) \le 900$	0	82.1091	-4.4838E-04	5.8961E-08	-2.4700E-10
	Si[3]	0	127.5	-4.9412E-05	-3.4510E-08	0
	$Ti-6Al-4V$ (Kim 2005)	0	122.70	-4.605E-4	0	0
	ZrO_2 (Kim 2005)	0	132.20	-3.805E-4	-6.127E-8	
υ	Al[2]	0	0.35			
	Si (Ansari *et al*. 2015)	0	0.24			
	$Ti-6Al-4V$ (Kim 2005)	0	0.2888	1.108E-4	0	0
	ZrO_2 (Kim 2005)	0	0.3330	0	0	0
$\rho(Kg/m^3)$	Al [1] $0 \le T(K) \le 922$	0	2727.2075	-3.2641E-05	1.6233E-08	-6.1935E-11
	Si (Hull 1999)	$0.2845103E4 - 0.1690\,T - 0.1750E - 3(T - 0.1687E4)^2$				
	$Ti-6Al-4V$ (Kim 2005)	0	4420	0	0	0
	ZrO_2 (Kim 2005)	0	3657	0	0	0
$\alpha\,(10^{-6}/K)$	Al[1,4] $25 \le T \le 900$	0	-2.1855	-7.0705E-02	1.2740E-04	-7.9704E-08
	Si (Hull 1999)	$0.3725E-5 - 0.3725E-5\,exp(-0.588E-2\,T + 0.72912) + 0.5548E-9\,T$				
	$Ti-6Al-4V$ (Kim 2005)	0	7.4300E-6	7.483E-4	-3.621E-7	0
	ZrO_2 (Kim 2005)	0	13.300E-6	-1.421E-3	9.549E-7	0
$\kappa(W/m\,K)$	Al[1,4] $0 \le T \le 933.52$	0	203.1537	1.0696E-03	-1.8995E-06	8.3775E-10
	Si [1] (Hull 1999) $200 \le T \le 1681$	0	412.0898	-2.5104E-03	2.1914E-06	-6.1993E-10
	$Ti-6Al-4V$ (Kim 2005)	0	6.1	0	0	0
	ZrO_2 (Kim 2005)	0	1.78	0	0	0
$\tau_0(N/m)$	Al[4]	0	1.0098	-1.5052E-04	-	-
	Si (Hull 1999)	0	1.2461	-1.7655E-04	-	-
$\lambda_0(N/m)$	Al[5]	0	6.842	0	0	0
	Si[5]	0	-4.488	0	0	0
$\mu_0(N/m)$	Al[5]	0	-0.376	0	0	0
	Si[5]	0	-2.774	0	0	0
$\rho_0(kg/m^2)$	Al[6]	0	5.46E-7	0	0	0
	Si[6]	0	3.17E-7	0	0	0

[1] The material property is obtained by the use of curve fitting method
[2] (Mondolfo 2013)
[3] (Swarnakar *et al*. 2014)
[4] (Aluminum Association 1984)
[5] (Shaat *et al*. 2013)
[6] (Ansari *et al*. 2015)

2.3 Strain-displacement relations

Based on the von Karman's theory and using Eqs. (6.1)-(6.3), the nonlinear strain-displacement relations are

$$\begin{cases} \varepsilon_{ij} = \varepsilon_{ij}^{0} + z\,\varepsilon_{ij}^{(1)} - z^3\varepsilon_{ij}^{(3)} & i,j = x,y \\ \varepsilon_{ij} = \varepsilon_{ij}^{0} + z^2\varepsilon_{ij}^{(2)} & i = x,y\,;\, j = z \end{cases} \tag{7}$$

Where

$$\begin{aligned} \varepsilon_{xx}^{0} &= \frac{1}{2}\left(\frac{\partial w_0}{\partial x}\right)^2 + \frac{\partial u_0}{\partial x} & \varepsilon_{xx}^{(1)} &= \frac{\partial \varphi_x}{\partial x} & \varepsilon_{xx}^{(3)} &= \frac{4}{3h^2}\left(\frac{\partial \varphi_x}{\partial x} + \frac{\partial^2 w_0}{\partial x^2}\right) \\ \varepsilon_{yy}^{0} &= \frac{1}{2}\left(\frac{\partial w_0}{\partial y}\right)^2 + \frac{\partial v_0}{\partial y} & \varepsilon_{yy}^{(1)} &= \frac{\partial \varphi_y}{\partial y} & \varepsilon_{xx}^{(3)} &= \frac{4}{3h^2}\left(\frac{\partial \varphi_y}{\partial y} + \frac{\partial^2 w_0}{\partial y^2}\right) \\ \varepsilon_{xy}^{0} &= \frac{1}{2}\left(\frac{\partial u_0}{\partial y} + \frac{\partial v_0}{\partial x} + \frac{\partial w_0}{\partial x}\frac{\partial w_0}{\partial y}\right) & \varepsilon_{xy}^{(1)} &= \frac{1}{2}\left(\frac{\partial \varphi_x}{\partial y} + \frac{\partial \varphi_y}{\partial x}\right) & \varepsilon_{xy}^{(3)} &= \frac{2}{3h^2}\left(\frac{\partial \varphi_x}{\partial y} + \frac{\partial \varphi_y}{\partial x}\right) + \frac{4}{3h^2}\frac{\partial^2 w_0}{\partial x \partial y} \\ \varepsilon_{xz}^{0} &= \frac{1}{2}\left(\varphi_x + \frac{\partial w_0}{\partial x}\right) & \varepsilon_{xz}^{(2)} &= -\frac{2}{h^2}\left(\varphi_x + \frac{\partial w_0}{\partial x}\right) \\ \varepsilon_{yz}^{0} &= \frac{1}{2}\left(\varphi_y + \frac{\partial w_0}{\partial y}\right) & \varepsilon_{yz}^{(2)} &= -\frac{2}{h^2}\left(\varphi_y + \frac{\partial w_0}{\partial y}\right) \end{aligned} \tag{8}$$

2.4 Nonlocal elasticity theory

The classical elasticity theory of its all ability, cannot explain some phenomena such as infinite stress at the tip of a sharp crack; nonlocal elasticity theory is one of those solutions which developed to describe phenomena like this (Ebrahimi, *et al.* 2016, Ebrahimi and Barati 2017c). In this theory, Eringen (1983, 1972) states: "the stress at a reference point x in the body depends not only on the strains at x but also on strains at all other points of the body"; this dependency between stresses can be stated as

$$\sigma_{ij}^{nl}(\boldsymbol{x}) = \int_V \alpha(|\boldsymbol{x}' - \boldsymbol{x}|, \tau)\sigma_{ij}^{cl}(\boldsymbol{x}')dv(\boldsymbol{x}') \tag{9}$$

Where $\sigma_{ij}^{nl}(\boldsymbol{x})$ is nonlocal stress at a reference point $\boldsymbol{x}$ in the body, $\sigma_{ij}^{cl}(\boldsymbol{x}')$ is macroscopic or classical stress at any point $(\boldsymbol{x}')$ in the body $(v(\boldsymbol{x}'))$ and $\alpha(|\boldsymbol{x}' - \boldsymbol{x}|, \tau)$ is Green's function which is called nonlocal modulus. The corresponding differential operator for two-dimensional nonlocal modulus is

$$\mathbf{L} = 1 - \mu\nabla^2 \tag{10}$$

Where μ is nonlocal parameter and ∇^2 is the Laplacian operator.

From Green's function theory (Duffy 2015) it is concluded

$$(1 - \mu\nabla^2)\sigma_{ij}^{nl} = \sigma_{ij}^{cl} \tag{11}$$

2.5 Stress-strain relations including surface effect

The surface stress is defined as a reversible work per area to stretch a surface elastically; it can also be defined mathematically as (Ibach 1997)

$$S_{ij} = \int_{-\infty}^{+\infty} \left(\sigma_{ij}(z) - \sigma_{ij}^{b}\right)dz \tag{12}$$

Where S_{ij} is surface stress tensor, $\sigma_{ij}(z)$ is bulk stress tensor as a function of z and σ_{ij}^{b} is the bulk stress in the vicinity of the surface which may be different from $\sigma_{ij}(z)$.

Eq. (12) denotes that surface stress not only is dependent to material behavior in the vicinity of surface but it is dependent to material behavior throughout the body of the material. It can be concluded that surface stresses become more important when surface to volume ratio rises.

Gurtin and Murdoch (1975, 1978) showed that surface stress is related to strain as

$$\frac{\partial S_{ij}}{\partial x_j} = \sigma_{ij}n_j + \rho_0\ddot{u}_i \qquad i,j = x,y,z \tag{13.1}$$

$$S_{ij} = \tau_0\delta_{ij} + 2(\mu_0 - \tau_0)E_{ij} + (\lambda_0 + \tau_0)E_{kk}\delta_{ij} + \tau_0\frac{\partial u_i}{\partial x_j} + o(\varepsilon) \tag{13.2}$$

$$S_{iz} = \tau_0\frac{\partial u_z}{\partial x_i} \qquad i,j = x,y \tag{13.3}$$

In above equations S_{ij} and E_{ij} are surface stress and strain tensor on surface region; $\rho_0, \tau_0, \lambda_0$ and μ_0 denote mass density, residual stress and Lame moduli of the surface, n_j is normal to surface, u_i and x_j are displacement and coordinate in the i and j directions and σ_{ij} is stress tensor in the body; meanwhile, nonlinear terms are accumulated in $o(\varepsilon)$.

The surface, effects on the body in two ways:

- Storing Strain energy in the surface: it is accounted in Hamilton's principle relation.

- Providing a distribution of stresses that is normal to the surface (herein, σ_z^{nl})

The later distribution is usually assumed linear through the thickness of the plate (Lu *et al.* 2006) however any distribution function, such as $f(z)$ shall verify the relation as

$$0 = \frac{\int_{-\frac{h}{2}}^{\frac{h}{2}} f(z)dz}{h} \qquad where \quad h = thickness\ of\ the\ plate$$

In the result of this distribution we have

$$\sigma_z^{nl} = f(z)\{(\tau_0^+ + \tau_0^-)(w_{,xx} + w_{,yy} - (\rho_0^- + \rho_0^+)\ddot{w})\} + \frac{1}{2}\{(\tau_0^+ - \tau_0^-)(w_{,xx} + w_{,yy} + (\rho_0^- - \rho_0^+)\ddot{w})\}$$

Where, w is displacement in z direction.

Anyway, after applying the nonlocal differential operator (Eq. (10)) to governing equations (in section 0) we will require the classical constitutive relation as

$$\sigma_{ij}^{cl} = \frac{E}{1+\upsilon}\left(\varepsilon_{ij} + \frac{\upsilon}{1-\upsilon}\varepsilon_{kk}\delta_{ij}\right) + \frac{\upsilon}{1-\upsilon}\sigma_z^{cl}\delta_{ij} \tag{16}$$

Where, E, υ and δ are respectively Young's modulus, Poisson's ratio and Kronecker delta.

2.6 Hygrothermal effects

The temperature variation produces a thermal expansion or contraction of the material and in the result thermal stresses are created. The classic thermal constitutive equation for an isotropic material in two-dimensional system is (Shen 2016, Bloom and Coffin 2000, Reddy 2006)

$$\sigma_x^T = \sigma_y^T = \frac{E}{1-\upsilon}\,\alpha\,\Delta T \qquad \sigma_{xy}^T = 0 \tag{17}$$

Where α is coefficient of thermal expansion (CTE).

In addition, like other composite materials, FG materials can absorb moisture. This moisture change leads to swelling strains and stresses analogous to thermal effects (Berthelot 2012). Similar to thermal effects, the classic moisture constitutive equation for an isotropic material in two-dimensional system is

$$\sigma_x^c = \sigma_y^c = \frac{E}{1-\upsilon}\,\beta\,\Delta C \qquad \sigma_{xy}^c = 0 \tag{18}$$

Where C is the relative mass moisture concentration as (Vasiliev and Morozov 2013)

$$C = \frac{\Delta m}{m} \tag{19}$$

Where Δm is mass increase after moisture absorption and m is the mass of the nano-plate; β is coefficient of moisture expansion (CME).

In the present paper, we study the situation where moisture absorption is related to ceramic and we neglect the moisture absorption by metal; it is also assumed β (CME of ceramic) is constant through the thickness and the amount of β and C are around the ceramic tiles values (Linht)

$$\beta = 60\ mm/m \qquad C = 3{\sim}6\% \tag{20}$$

2.7 Temperature and moisture distribution

It is assumed that the temperature and moisture distribution occurs in the thickness direction only and one-dimensional temperature and moisture field is assumed to be constant in the XY plane of the plate.

For steady-state situation the temperature distribution along the thickness can be obtained by

$$\frac{\mathrm{d}}{\mathrm{dz}}\left[\kappa_f(z,T)\frac{dT}{dz}\right] = 0 \tag{21}$$

Expanding of Eq. (21) gives

$$\frac{d\kappa_f(z,T)}{dz}\frac{dT}{dz} + \frac{d\kappa_f(z,T)}{dT}\left(\frac{dT}{dz}\right)^2 + \kappa_f(z,T)\frac{d^2T}{dz^2} = 0 \tag{22}$$

Linearizing of Eq. (22) delivered

$$\kappa_f(z,T)\frac{d^2T}{dz^2} + \frac{d\kappa_f(z,T)}{dz}\frac{dT}{dz} = 0 \tag{23}$$

The analytical solution to Eq. (23) is

$$T(z) = T_m + \Delta T_{cm}\frac{\int_{-\frac{h}{2}}^{z}\frac{dz}{\kappa_f(z,T)}}{\int_{-\frac{h}{2}}^{h/2}\frac{dz}{\kappa_f(z,T)}} \tag{24.1}$$

Where

$$\Delta T_{cm} = T_c - T_m \tag{24.2}$$

From Eq. (24.1) the temperature rise can be calculated as (Ebrahimi and Barati 2016b, Ebrahimi and Barati 2016c)

$$\Delta T = T(z) - T_0 = (T_m - T_0) + \Delta T_{cm}\frac{\int_{-\frac{h}{2}}^{z}\frac{dz}{\kappa_f(z,T)}}{\int_{-\frac{h}{2}}^{h/2}\frac{dz}{\kappa_f(z,T)}} \tag{25}$$

Where T_0 is initial temperature. If $\kappa_f(z,T)$ is constant or variant, the temperature rise will be linear or nonlinear (Javaheri and Eslami 2002). From Eq. (25), it is visible that for calculating ΔT, we should find $T(z)$ by using Eq. (24.1), first. For linear assumption the temperature distribution is (Ebrahimi and Barati 2018b)

$$T(z) = T_m + \Delta T_{cm}\frac{(z + h/2)}{h} \tag{26}$$

For nonlinear situation, Eq. (24.1) is solved using iterative method for at every z; first we set $T = \frac{T_m + T_c}{2}$; second we calculate $\kappa_f(z,T)$ using Eq. (3.4); then the new T is calculated from Eq. (24.1); the procedure is repeated until convergence is reached.

Analogous to temperature distribution, Fick's law as (Vasiliev and Morozov 2013)

$$\frac{\mathrm{d}}{\mathrm{dz}}\left(D(z,T)\frac{dC}{dz}\right) = 0 \tag{27}$$

can be used to calculate one-dimensional moisture field, through the thickness of the plate under steady state situation, where $D(z,T)$ is diffusion coefficient.

Herein, we assume $D(z,T) = constant$, this means the moisture rise is linear and Similar to Eq. (26) the moisture distribution is

$$C(z) = C_m + \Delta C_{cm}\frac{(z+h/2)}{h} \qquad where \qquad \Delta C_{cm} = C_c - C_m \tag{28}$$

It is concluded that

$$\Delta C = C(z) - C_0 = (C_m - C_0) + \Delta C_{cm}\frac{(z+h/2)}{h} \tag{29}$$

3. Governing equations

By using Hamilton's principle as below (Abdelaziz *et al.* 2017, Meziane *et al.* 2014, Kaci *et al.* 2018, Ebrahimi and Barati 2017d, Ebrahimi and Heidari 2017)

$$0 = \int_0^{t_0} (\delta U + \delta V - \delta K)\, dt \tag{30}$$

the governing equation can be driven; in this equation U is the strain energy, V is the work done by environment, K is the kinetic energy and δ is the first variational operator.

The variation of strain energy is divided into two parts

$$\delta U = \delta U_b + \delta U_s \tag{31.1}$$

Where δU_b and δU_s are respectively the variation of strain energy and surface strain energy and are expressed as (Reddy 2006, Ansari *et al.* 2014)

$$\delta U_b = \int_\Omega \int_{-\frac{h}{2}}^{\frac{h}{2}} \left(\sigma_{xx}^{nl}\delta\varepsilon_{xx} + \sigma_{yy}^{nl}\delta\varepsilon_{yy} + 2\sigma_{xy}^{nl}\delta\varepsilon_{xy} + 2\sigma_{xz}^{nl}\delta\varepsilon_{xz} + 2\sigma_{yz}^{nl}\delta\varepsilon_{yz}\right) dz\, dx\, dy \tag{31.2}$$

$$\begin{aligned}\delta U_s &= \delta U_s^+ + \delta U_s^- \\ &= \int_\Lambda \Big((S_{xx}^{nl+} + S_{xx}^{nl-})\delta\varepsilon_{xx} \\ &+ \left(S_{xy}^{nl+} + S_{yx}^{nl+} + S_{xy}^{nl-} + S_{yx}^{nl-}\right)\delta\varepsilon_{xy} \\ &+ \left(S_{yy}^{nl+} + S_{yy}^{nl-}\right)\delta\varepsilon_{yy} \\ &+ 2\left((S_{xz}^{nl+} + S_{xz}^{nl-})\right)\delta\varepsilon_{xz} \\ &+ 2\left(S_{yz}^{nl+} + S_{yz}^{nl-}\right)\delta\varepsilon_{yz}\Big)\, dx\, dy\end{aligned} \tag{31.3}$$

Where in above equations superscripts "+" and "-" denote upper and lower surface of the nano-plate; Ω and Λ denote, respectively, the undeformed middle plane of the plate and the undeformed surface layer of the plate.

The second term in Eq. (30) is related to interaction between the nano-plate and its surrounding environment; the interaction between a system (herein, the nano-plate) takes place in different ways, one of them is thermal interaction; the work done by thermal interactions is (Praveen and Reddy 1998)

$$\begin{aligned}\delta V^T &= -\int_\Omega \int_{-\frac{h}{2}}^{\frac{h}{2}} \sigma_{ij}^{T,nl}\delta\varepsilon_{ij} dz\, dx\, dy \\ &= -\int_\Omega \int_{-\frac{h}{2}}^{\frac{h}{2}} \left(\sigma_x^{T,nl}\delta\varepsilon_x + \sigma_y^{T,nl}\delta\varepsilon_y\right) dz\, dx\, dy\end{aligned} \tag{32}$$

Where $\sigma_{ij}^{T,nl}$ is nonlocal thermal stress tensor.

The moisture diffusion is another interaction between a system and environment which the work of, is

$$\begin{aligned}\delta V^c &= -\int_\Omega \int_{-\frac{h}{2}}^{\frac{h}{2}} \sigma_{ij}^{c,nl}\delta\varepsilon_{ij} dz\, dx\, dy \\ &= -\int_\Omega \int_{-\frac{h}{2}}^{\frac{h}{2}} \left(\sigma_x^{c,nl}\delta\varepsilon_x + \sigma_y^{c,nl}\delta\varepsilon_y\right) dz\, dx\, dy\end{aligned} \tag{33}$$

Where $\sigma_{ij}^{c,nl}$ is nonlocal moisture stress tensor.

The interaction between a system and environment can be done through external forces; the work done by external forces is (Reddy 2006)

$$\begin{aligned}\delta V^e = -\int_\Omega &\left(q - K_w w_0 + K_p\nabla^2 w_0\right)\delta w_0\, dx\, dy \\ &- \int_{\Gamma_\sigma} \Big(\hat{N}_{nn}\delta u_{0n} + \hat{M}_{nn}\delta\varphi_n \\ &- \frac{4}{3h^2}\hat{P}_{nn}\delta\psi_n + \hat{N}_{ns}\delta u_{0s} \\ &+ \hat{M}_{ns}\delta\varphi_s - \frac{4}{3h^2}\hat{P}_{ns}\delta\psi_s \\ &+ \hat{Q}_n\delta w_0\Big)\, d\Gamma\end{aligned} \tag{34}$$

Where $q(x,y)$ is resultant of distributed transverse loads applied at the top and bottom surface of the nano-plate, $\hat{\sigma}_{nn}$ *and* $\hat{\sigma}_{ns}$ are, respectively, inplane normal and tangential stress acting on the boundary of the plate, $\hat{\sigma}_{nz}$ is the transverse shear stress acting on the portion Γ_σ of the boundary of the plate, K_w and K_p are respectively, Winkler and Pasternak modulus of elastic foundation (Jung *et al.* 2014, Yazid *et al.* 2018, Bounouara *et al.* 2016, Khetir *et al.* 2017, Besseghier *et al.* 2017, Mouffoki *et al.* 2017, Ebrahimi

and Shafiei 2017), Γ is the boundary of the plate and

$$\begin{Bmatrix} \widehat{N}_{ij} \\ \widehat{M}_{ij} \\ \widehat{P}_{ij} \end{Bmatrix} = \int_{-\frac{h}{2}}^{\frac{h}{2}} \hat{\sigma}_{ij} \begin{Bmatrix} 1 \\ z \\ z^3 \end{Bmatrix} dz \quad \hat{Q}_n = \int_{-\frac{h}{2}}^{\frac{h}{2}} \hat{\sigma}_{nz} dz \quad \hat{Q}_n = \int_{-\frac{h}{2}}^{\frac{h}{2}} \hat{\sigma}_{nz} dz \tag{35}$$

Finally, the variation of the work done by environment is

$$\delta V = \delta V^T + \delta V^c + \delta V^e \tag{36}$$

The variation of the kinetic energy is (Reddy 2006)

$$\begin{aligned} \delta K = \int_\Omega \Big\{ & \Big(I_0 \dot{u}_0 + I_1 \dot{\varphi}_x - \frac{4I_3}{3h^2} \dot{\psi}_x \Big) \delta \dot{u}_0 \\ & + \Big(I_0 \dot{v}_0 + I_1 \dot{\varphi}_y - \frac{4I_3}{3h^2} \dot{\psi}_y \Big) \delta \dot{v}_0 \\ & + \Big(I_1 \dot{u}_0 + I_2 \dot{\varphi}_x - \frac{4I_4}{3h^2} \dot{\psi}_x \Big) \delta \dot{\varphi}_x \\ & + \Big(-\frac{4I_3}{3h^2} \dot{u}_0 - \frac{4I_4}{3h^2} \dot{\varphi}_x \\ & + \frac{16I_6}{9h^4} \dot{\psi}_x \Big) \delta \dot{\psi}_x \\ & + \Big(I_1 \dot{v}_0 + I_2 \dot{\varphi}_y - \frac{4I_4}{3h^2} \dot{\psi}_y \Big) \delta \dot{\varphi}_y \\ & + \Big(-\frac{4I_3}{3h^2} \dot{v}_0 - \frac{4I_4}{3h^2} \dot{\varphi}_y \\ & + \frac{16I_6}{9h^4} \dot{\psi}_y \Big) \delta \dot{\psi}_y \\ & + I_0 \dot{w}_0 \delta \dot{w}_0 \Big\} \, dx \, dy \end{aligned} \tag{37}$$

Where

$$I_i = \int_{-\frac{h}{2}}^{\frac{h}{2}} \rho z^i dz \quad \psi_j = \varphi_j - z \frac{\partial w_0}{\partial j} = \delta\varphi_j - z \frac{\partial \delta w_0}{\partial j} \tag{38}$$

By substituting Eqs. (31), (36) and (37) into Hamilton's principle (Eq. (30)) and applying the nonlocal differential operator (Eq. (10)), the governing equations of motion can be obtained as

$$\delta u_0: \quad \begin{aligned} & \bar{N}_{xx,x} + \bar{N}_{xy,y} = I_0 \mathbf{L}\ddot{u}_0 - I_{13} \mathbf{L}\ddot{\varphi}_x \\ & - \frac{4I_3}{3h^2} \mathbf{L}\ddot{w}_{0,x} \end{aligned} \tag{1.1}$$

$$\delta v_0: \quad \begin{aligned} & \bar{N}_{yy,y} + \bar{N}_{xy,x} = I_0 \mathbf{L}\ddot{v}_0 - I_{13} \mathbf{L}\ddot{\varphi}_y \\ & - \frac{4I_3}{3h^2} \mathbf{L}\ddot{w}_{0,y} \end{aligned} \tag{1.2}$$

$$\delta\varphi_x: \quad \begin{aligned} & -\bar{M}_{xx,x} - \bar{M}_{xy,y} + \frac{4}{3h^2}\left(\bar{P}_{xx,x} + \bar{P}_{xy,y}\right) + \bar{Q}_x \\ & = I_{13} \mathbf{L}\ddot{u}_0 + I_{246} \mathbf{L}\ddot{\varphi}_x \\ & + I_{46} \mathbf{L}\ddot{w}_{0,x} \end{aligned} \tag{1.3}$$

$$\delta\varphi_y: \quad \begin{aligned} & -\bar{M}_{yy,y} - \bar{M}_{xy,x} + \frac{4}{3h^2}\left(\bar{P}_{yy,y} + \bar{P}_{xy,x}\right) + \bar{Q}_y \\ & = I_{13} \mathbf{L}\ddot{v}_0 + I_{246} \mathbf{L}\ddot{\varphi}_y \\ & + I_{46} \mathbf{L}\ddot{w}_{0,y} \end{aligned} \tag{1.4}$$

$$\delta w_0: \quad \begin{aligned} & -\frac{4}{3h^2}\left(\bar{P}_{xx,xx} + \bar{P}_{yy,yy} + 2\bar{P}_{xy,xy}\right) \\ & - \mathbf{L}\left(\bar{\mathbb{N}}^{nl}(u_0, v_0, w_0)\right) \\ & - \bar{Q}_{x,x} - \bar{Q}_{y,y} \\ & - K_p \mathbf{L}\nabla^2 w_0 + K_w \mathbf{L} w_0 \\ & = -I_0 \mathbf{L}\ddot{w}_0 - \frac{4I_3}{3h^2}\left(\mathbf{L}\ddot{u}_{0,x} + \mathbf{L}\ddot{v}_{0,y}\right) \\ & - I_{46}\left(\mathbf{L}\ddot{\varphi}_{x,x} + \mathbf{L}\ddot{\varphi}_{y,y}\right) \\ & + \frac{16I_6}{9h^4} \mathbf{L}\nabla^2 \ddot{w}_0 \end{aligned} \tag{1.5}$$

With boundary condition as

$$\delta u_{0n} = 0 \text{ or } \bar{N}_{nn} = \hat{N}_{nn} \tag{2.1}$$

$$\delta u_{0s} = 0 \text{ or } \bar{N}_{ns} = \hat{N}_{ns} \tag{2.2}$$

$$\delta w_0 = 0 \text{ or } \bar{V}_n = \hat{V}_n \tag{2.3}$$

$$\delta\varphi_n = 0 \text{ or } \begin{matrix} \bar{M}_{nn} \\ -\frac{4}{3h^2}\bar{P}_{nn} \\ = \hat{M}_{nn} \\ -\frac{4}{3h^2}\hat{P}_{nn} \end{matrix} \tag{2.4}$$

$$\delta\varphi_s = 0 \text{ or } \begin{matrix} \bar{M}_{ns} \\ -\frac{4}{3h^2}\bar{P}_{ns} \\ = \hat{M}_{ns} \\ -\frac{4}{3h^2}\hat{P}_{ns} \end{matrix} \tag{2.5}$$

$$\frac{\partial \delta w_0}{\partial n} = 0 \text{ or } \bar{P}_{nn} = \hat{P}_{nn} \tag{2.6}$$

Where

$$\begin{aligned} \bar{\mathbb{N}}^{nl}(u_0, v_0, w_0) = & \left(\bar{N}^{nl}_{xx} w_{0,x} + \bar{N}^{nl}_{xy} w_{0,y}\right)_{,x} \\ & + \left(\bar{N}^{nl}_{yy} w_{0,y} + \bar{N}^{nl}_{xy} w_{0,x}\right)_{,y} \end{aligned} \tag{3.1}$$

$$\bar{A}_{ij} = A_{ij} + A_{ij}^{s} - A_{ij}^{T} - A_{ij}^{c} \qquad A = N, M, P \quad i = x, y \tag{3.2}$$

$$\left[N_{ij}, M_{ij}, P_{ij}\right] = \int_{-\frac{h}{2}}^{\frac{h}{2}} \sigma_{ij}[1, z, z^3]\, dz \qquad i = x, y \tag{3.3}$$

$$\left[N_{ij}^{\zeta}, M_{ij}^{\zeta}, P_{ij}^{\zeta}\right] = \int_{-\frac{h}{2}}^{\frac{h}{2}} \sigma_{ij}^{\zeta}[1, z, z^3]\, dz \qquad \zeta = c, T \tag{3.4}$$

$$\bar{A}_i = A_i + A_i^{s} \qquad A = Q, R \tag{3.5}$$

$$[Q_i, R_i] = \int_{-\frac{h}{2}}^{\frac{h}{2}} \sigma_{iz}[1, z^2]\, dz \qquad i = x, y \tag{3.6}$$

$$\begin{Bmatrix} N_{ij}^{s} \\ M_{ij}^{s} \\ P_{ij}^{s} \end{Bmatrix} = \begin{Bmatrix} \frac{\left(S_{ij}^{+} + S_{ji}^{+} + S_{ij}^{-} + S_{ji}^{-}\right)}{2} \\ \left(S_{ij}^{+} + S_{ji}^{+} - S_{ij}^{-} - S_{ji}^{-}\right)\frac{h}{4} \\ \frac{\left(S_{ij}^{+} + S_{ji}^{+} - S_{ij}^{-} - S_{ji}^{-}\right)}{2}\left(\frac{h}{2}\right)^3 \end{Bmatrix} \quad \begin{Bmatrix} Q_i^{s} \\ R_i^{s} \end{Bmatrix} = \begin{Bmatrix} S_{iz}^{+} + S_{iz}^{-} \\ \left(S_{iz}^{+} + S_{iz}^{-}\right)\left(\frac{h}{2}\right)^2 \end{Bmatrix} \tag{3.7}$$

$$\hat{V}_n = \hat{Q}_n + \frac{4}{3h^2}\frac{\partial \hat{P}_{ns}}{\partial s} \qquad \hat{Q}_n = \int_{-\frac{h}{2}}^{\frac{h}{2}} \hat{\sigma}_{nz} dz \tag{3.8}$$

$$\bar{V}_n = \mathbf{L}\, \bar{V}_n^{nl} \tag{3.9}$$

$$\bar{V}_n^{nl} = \mathcal{F}^{nl}(u_0, v_0, w_0) + \frac{4}{3h^2}\left(\bar{P}_{xx,x}^{nl} + \bar{P}_{xy,y}^{nl}\right)n_x + \frac{4}{3h^2}\left(\bar{P}_{yy,y}^{nl} + \bar{P}_{xy,x}^{nl}\right)n_y + \bar{Q}_x^{nl} n_x + \bar{Q}_y^{nl} n_y - \left(I_{46}\ddot{\varphi}_y - \frac{16I_6}{9h^4}\ddot{w}_{0,y}\right)n_y - \left(I_{46}\ddot{\varphi}_x - \frac{16I_6}{9h^4}\ddot{w}_{0,x}\right)n_x - \frac{4I_3}{3h^2}\ddot{u}_0 n_x - \frac{4I_3}{3h^2}\ddot{v}_0 n_y + \frac{4}{3h^2}\frac{\partial \bar{P}_{ns}^{nl}}{\partial s} \tag{3.10}$$

$$I_{13} = \frac{4I_3}{3h^2} - I_1 \qquad I_{246} = -I_2 + \frac{8I_4}{3h^2} - \frac{16I_6}{9h^4} \qquad I_{46} = \frac{4I_4}{3h^2} - \frac{16I_6}{9h^4} \tag{3.11}$$

Eq. (3.1) can be linearized as (Reddy 2010)

$$\bar{\mathrm{N}}^{nl}(u_0, v_0, w_0) \approx \bar{N}_{xx}^{nl} w_{0,xx} + 2\bar{N}_{xy}^{nl} w_{0,xy} + \bar{N}_{yy}^{nl} w_{0,yy} \tag{42}$$

in the result we can conclude

$$\mathbf{L}\left(\bar{\mathrm{N}}^{nl}(u_0, v_0, w_0)\right) \approx \bar{N}_{xx} w_{0,xx} + 2\bar{N}_{xy} w_{0,xy} + \bar{N}_{yy} w_{0,yy} \tag{43}$$

To solve the governing equations (Eqs. (1.1)-(1.5)), after using the relations in section (0) we set

$$\begin{Bmatrix} u_0(x,y,t) \\ v_0(x,y,t) \\ w_0(x,y,t) \\ \varphi_x(x,y,t) \\ \varphi_y(x,y,t) \end{Bmatrix} = \begin{Bmatrix} U_0(x,y) \\ V_0(x,y) \\ W_0(x,y) \\ \Phi_x(x,y) \\ \Phi_y(x,y) \end{Bmatrix} e^{j\omega t} \tag{44}$$

the resulting non-dimensionlized governing equations are

$$\begin{aligned} &D21\, W_{0,YYY} + D12\, W_{0,XYY} + D14\, \Phi_{X,XX} \\ &\quad + D15\, \Phi_{X,YY} + \\ &+D16\, \Phi_{Y,XY} + D17 U_{0,XX} + D18\, U_{0,YY} \\ &\quad + D19\, V_{0,XY} + D111\, W_{0,X} W_{0,XX} \\ &\quad + \\ &+D112\, W_{0,Y} W_{0,XY} + D113\, W_{0,X} W_{0,YY} \\ &\quad + \\ &+\lambda^2 (F11\, W_{0,X} + F12 U_{0,XX} \\ &\quad + F13 U_{0,YY} + F14\, U_0 + F15\, \Phi_X \\ &\quad + \\ &+F16\, W_{0,XXX} + F17\, W_{0,XYY} \\ &\quad + F18\, \Phi_{X,XX} + F19\, \Phi_{X,YY}) = 0 \end{aligned} \tag{4.1}$$

$$\begin{aligned} &D21\, W_{0,YYY} + D22\, W_{0,XXY} + D24\, \Phi_{X,XY} \\ &\quad + D25\, \Phi_{Y,XX} + D26\, \Phi_{Y,YY} \\ &\quad + D27\, U_{0,XY} + \\ &+D28\, V_{0,XX} + D210\, V_{0,YY} \\ &\quad + D211\, W_{0,Y} W_{0,XX} \\ &\quad + D212\, W_{0,X} W_{0,XY} + \\ &+D213\, W_{0,Y} W_{0,YY} + \lambda^2 (F21\, V_{0,XX} \\ &\quad + F22\, V_{0,YY} + F23\, W_{0,Y} \\ &\quad + F24\, V_0 + \\ &+F25\, W_{0,YYY} + F26\, W_{0,XXY} \\ &\quad + F27\, \Phi_{Y,XX} + F28\, \Phi_{Y,YY} \\ &\quad + F29\, \Phi_Y) = 0 \end{aligned} \tag{4.2}$$

$$\begin{aligned} &D31\, W_{0,XXX} + D32\, W_{0,XYY} + D35\, W_{0,X} \\ &\quad + D36\, \Phi_{X,XX} + D37\, \Phi_{X,YY} \\ &\quad + D38\, \Phi_X + \\ &+D39\, \Phi_{Y,XY} + D311\, U_{0,XX} \\ &\quad + D312\, U_{0,YY} + D313\, V_{0,XY} + \\ &+D314\, W_{0,X} W_{0,XX} \\ &\quad + D315\, W_{0,Y} W_{0,XY} \\ &\quad + D316\, W_{0,X} W_{0,YY} + \\ &+\lambda^2 (F31\, \Phi_{X,XX} + F32\, \Phi_{X,YY} \\ &\quad + F33\, W_{0,XXX} + F34\, W_{0,XYY} \\ &\quad + F35\, W_{0,X} + \\ &+F36\, \Phi_X + F37\, U_{0,XX} + F38\, U_{0,YY} \\ &\quad + F39\, U_0) = 0 \end{aligned} \tag{4.3}$$

$$
\begin{aligned}
&D41\,W_{0,YYY} + D42\,W_{0,XXY} + D45\,W_{0,Y} \\
&\quad + D46\,\Phi_{X,XY} + D47\,\Phi_{Y,XX} \\
&\quad + D49\,\Phi_Y + \\
&+D410\,\Phi_{Y,YY} + D411\,U_{0,XY} \\
&\quad + D412\,V_{0,XX} + D413\,V_{0,YY} + \\
&+D414\,W_{0,Y}\,W_{0,XX} \\
&\quad + D415\,W_{0,X}\,W_{0,XY} \\
&\quad + D416\,W_{0,Y}\,W_{0,YY} + \\
&+\lambda^2(F41\,\Phi_{Y,XX} + F42\,\Phi_{Y,YY} \\
&\quad + F43\,W_{0,XXY} + F44\,W_{0,YYY} \\
&\quad + F45\,W_{0,Y} + \\
&+F46\,\Phi_Y + F47\,V_{0,XX} + F48\,V_{0,YY} \\
&\quad + F49\,V_0) = 0
\end{aligned}
\tag{4.4}
$$

$$
\begin{aligned}
&D51\,W_{0,XXXX} + D52\,W_{0,YYYY} + D54\,W_{0,XXYY} \\
&\quad + D57\,W_{0,XX} + D58\,W_{0,YY} + \\
&+D547\,W_0 + D59\,\varphi_{X,XXX} \\
&\quad + D510\,\varphi_{X,XYY} + D511\,\varphi_{X,X} + \\
&+D512\,\varphi_{Y,YYY} + D513\,\varphi_{Y,XXY} \\
&\quad + D515\,\varphi_{Y,Y} + D516\,U_{0,XXX} + \\
&+D517\,U_{0,XYY} + D518\,V_{0,YYY} \\
&\quad + D519\,V_{0,XXY} + D520\,{W_{0,XX}}^2 + \\
&+D521\,{W_{0,XY}}^2 + D522\,{W_{0,YY}}^2 \\
&\quad + D523\,W_{0,X}W_{0,XXX} + \\
&+D525\,W_{0,XX}W_{0,YY} \\
&\quad + D526\,W_{0,Y}W_{0,YYY} \\
&\quad + D528\,W_{0,Y}W_{0,XXY} + \\
&+D529\,W_{0,X}W_{0,XYY} \\
&\quad + D530\,U_{0,X}W_{0,XX} \\
&\quad + D531\,U_{0,X}W_{0,YY} + \\
&+D532\,U_{0,Y}W_{0,XY} + D533\,V_{0,X}W_{0,XY} \\
&\quad + D534\,V_{0,Y}W_{0,XX} \\
&+D535\,V_{0,Y}W_{0,YY} + D536\,\Phi_{X,X}W_{0,YY} \\
&\quad + D537\,\Phi_{X,X}W_{0,XX} + \\
&+D538\,\Phi_{X,Y}W_{0,XY} \\
&\quad + D539\,W_{0,XX}\Phi_{Y,Y} \\
&\quad + D540\,\Phi_{Y,Y}W_{0,YY} + \\
&+D541\,\Phi_{Y,X}W_{0,XY} \\
&\quad + D542\,W_{0,X}W_{0,Y}W_{0,XY} + \\
&+D543\,{W_{0,X}}^2W_{0,XX} \\
&\quad + D544\,{W_{0,Y}}^2W_{0,XX} \\
&\quad + D545\,{W_{0,Y}}^2W_{0,YY} + \\
&+D546\,{W_{0,X}}^2W_{0,YY} \\
&\quad + \lambda^2(F51\,W_{0,XXXX} \\
&\quad + F52\,W_{0,XXYY} + \\
&+F53\,W_{0,YYYY} + F54\,W_{0,XX} \\
&\quad + F55\,W_{0,YY} + \\
&+F56\,W_0 + F57\,\Phi_{X,XXX} \\
&\quad + F58\,\Phi_{X,XYY} + F59\,\Phi_{Y,XXY} + \\
&+F510\,\Phi_{Y,YYY} + F511\,W_0W_{0,XX} \\
&\quad + F512\,W_0W_{0,YY} + \\
&+ + F513\,\Phi_{X,X} + F514\,\Phi_{Y,Y} + F515\,U_{0,XXX} \\
&\quad + F516\,U_{0,XYY} + \\
&+F517\,V_{0,XXY} + F518\,V_{0,YYY} + F519\,U_{0,X} \\
&\quad + F520\,V_{0,Y}) = 0
\end{aligned}
\tag{4.5}
$$

$$
\begin{aligned}
&D41\,W_{0,YYY} + D42\,W_{0,XXY} + D45\,W_{0,Y} \\
&\quad + D46\,\Phi_{X,XY} + D47\,\Phi_{Y,XX} \\
&\quad + D49\,\Phi_Y + \\
&+D410\,\Phi_{Y,YY} + D411\,U_{0,XY} \\
&\quad + D412\,V_{0,XX} + D413\,V_{0,YY} + \\
&+D414\,W_{0,Y}\,W_{0,XX} \\
&\quad + D415\,W_{0,X}\,W_{0,XY} \\
&\quad + D416\,W_{0,Y}\,W_{0,YY} + \\
&+\lambda^2(F41\,\Phi_{Y,XX} + F42\,\Phi_{Y,YY} \\
&\quad + F43\,W_{0,XXY} + F44\,W_{0,YYY} \\
&\quad + F45\,W_{0,Y} + \\
&+F46\,\Phi_Y + F47\,V_{0,XX} + F48\,V_{0,YY} \\
&\quad + F49\,V_0) = 0
\end{aligned}
\tag{45.6}
$$

In a same manner the non -dimensional resultant stresses are

$$
\begin{aligned}
\widetilde{N}_{XX} &= V71\,W_{0,XX} + V72\,W_{0,YY} + V74\,\Phi_{X,X} \\
&\quad + V75\,\Phi_{Y,Y} + V76\,U_{0,X} \\
&\quad + V77\,V_{0,Y} + \\
&+V78\,{W_{0,X}}^2 + V77\,V_{0,Y} + V78\,{W_{0,X}}^2 \\
&\quad + V79\,{W_{0,Y}}^2 + V711\,\lambda^2\,W_0 \\
&\quad + V710
\end{aligned}
\tag{46.1}
$$

$$
\begin{aligned}
\widetilde{N}_{YY} &= V91\,W_{0,XX} + V92\,W_{0,YY} + V94\,\Phi_{X,X} \\
&\quad + V95\,\Phi_{Y,Y} + V96U_{0,X} \\
&\quad + V97V_{0,Y} + \\
&+V98\,{W_{0,X}}^2 + V99\,{W_{0,Y}}^2 + V911\,\lambda^2\,W_0 \\
&\quad + V910
\end{aligned}
\tag{46.2}
$$

$$
\begin{aligned}
\widetilde{M}_{XX} &= V61\,W_{0,XX} + V62\,W_{0,YY} + V63\,\Phi_{X,X} \\
&\quad + V64\,\Phi_{Y,Y} + V65\,U_{0,X} \\
&\quad + V66\,V_{0,Y} + \\
&+V67\,W_{0,X}^2 + V68\,W_{0,Y}^2 + F61\,\lambda^2\,W_0 + V69
\end{aligned}
\tag{46.3}
$$

$$
\begin{aligned}
\widetilde{M}_{YY} &= V81\,W_{0,XX} + V82\,W_{0,YY} + V83\,\Phi_{X,X} \\
&\quad + V84\,\Phi_{Y,Y} + V85\,U_{0,X} \\
&\quad + V86\,V_{0,Y} + \\
&+V87\,W_{0,X}^2 + V88\,W_{0,Y}^2 + F81\,\lambda^2\,W_0 + V89
\end{aligned}
\tag{46.4}
$$

$$
\begin{aligned}
\tilde{P}_{XX} &= V101\,W_{0,XX} + V102\,W_{0,YY} + V104\,\Phi_{X,X} \\
&\quad + V105\,\Phi_{Y,Y} + V106\,U_{0,X} + \\
&+V107\,V_{0,Y} + V108\,W_{0,X}^2 + V109\,W_{0,Y}^2 \\
&\quad + V1010\,\lambda^2 W_0 + V1011
\end{aligned}
\tag{46.5}
$$

$$
\begin{aligned}
\tilde{P}_{YY} &= V12_1W_{0,XX} + V12_2W_{0,YY} + V12_4\Phi_{X,X} \\
&\quad + V12_5\Phi_{Y,Y} + V12_6U_{0,X} + \\
&+V12\_7\,V_{0,Y} + V12\_8\,W_{0,X}^2 + V12\_9\,W_{0,Y}^2 \\
&\quad + V12\_10\,\lambda^2\,W_0 + V12\_11
\end{aligned}
\tag{46.6}
$$

Dij,Vij and Fij coefficients are available in Appendix A.

Eqs. (46.1)-(46.6) are used in boundary condition equations; because $V710, V910, V69, V89, V1011$ and $V12\_11$ are negligible all boundary conditions can be considered as homogeneous.

Three boundary conditions are studied in the present study:

(a) All edges movable simply-supported (SSSS)

$$
\begin{aligned}
&V_0 = W_0 = \Phi_Y = \widehat{N}_{XX} = \widehat{M}_{XX} = \hat{P}_{XX} \\
&\quad = 0 \qquad at\ edges\ X = 0,1 \\
&U_0 = W_0 = \Phi_X = \widehat{N}_{YY} = \widehat{M}_{YY} = \hat{P}_{YY} \\
&\quad = 0 \qquad at\ edges\ Y = 0,1
\end{aligned}
\tag{5}
$$

(b) All edges clamped (CCCC)

$$
\begin{aligned}
&U_0 = V_0 = W_0 = \Phi_X = \Phi_Y = \frac{\partial W_0}{\partial X} \\
&\quad = 0 \qquad at\ edges\ X = 0,1 \\
&U_0 = V_0 = W_0 = \Phi_X = \Phi_Y = \frac{\partial W_0}{\partial Y} \\
&\quad = 0 \qquad at\ edges\ Y = 0,1
\end{aligned}
\tag{6}
$$

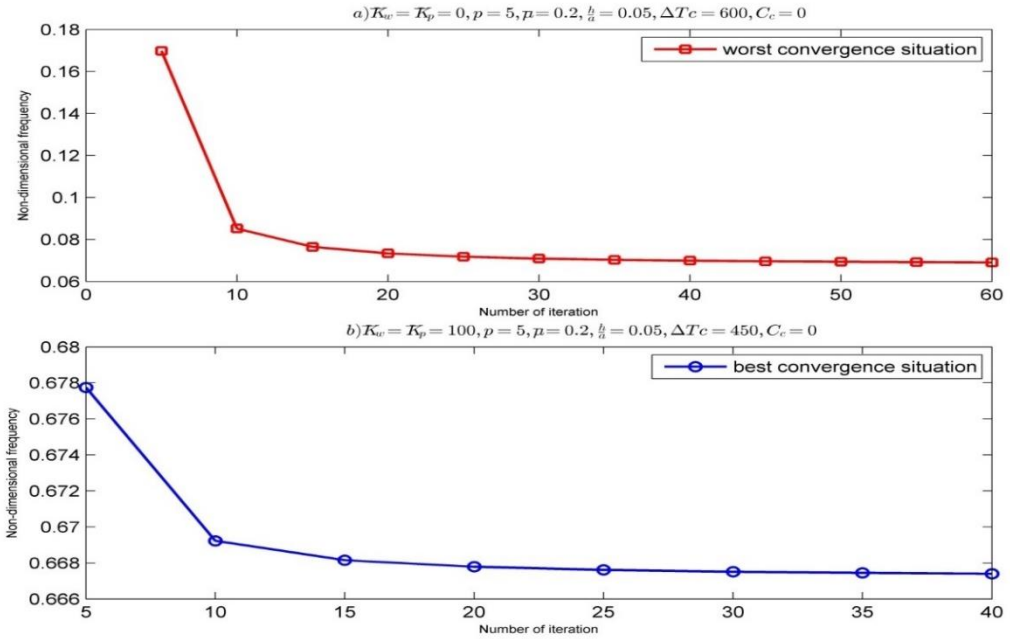

Fig. 2 Convergence comparing of dimensionless fundamental frequencies of Al/Si square FG Reddy nano-plate considering surface stresses effect $(\boldsymbol{a = 200\ nm, \lambda = \omega a \sqrt{\frac{\rho_c}{E_c}}})$

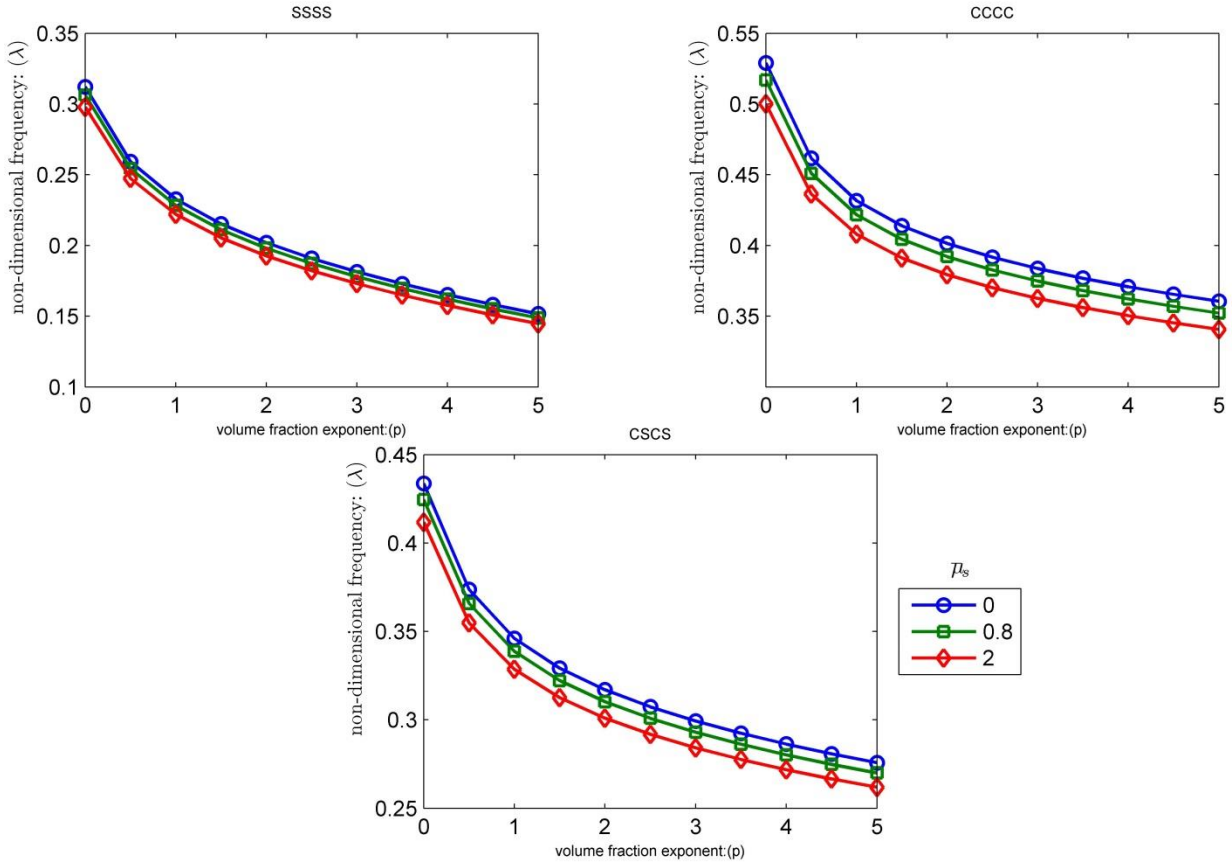

Fig. 3 Influence of nonlocal parameter on non-dimensional fundamental natural frequencies of square $(\boldsymbol{Al/Si})$ FG Reddy nano -plate with respect to various volume fraction exponent for different boundary conditions, considering surface stresses effect $(\boldsymbol{\bar{K}_w = \bar{K}_p = 0, h/a = 0.05, a = 200\ nm, \Delta T_c = 450\ K, \Delta C = C_c = 0})$

Table 2 Influence of nonlocal parameter on non – dimensional fundamental natural frequencies of square (Al/Si) FG Reddy nano-plate with respect to various volume fraction exponent for different boundary conditions, considering surface stresses effect ($\overline{K}_w = \overline{K}_p = 0, h/a = 0.05, a = 200\ nm, \Delta T_c = 450\ K, \Delta C = C_c = 0$)

		SSSS		CCCC		CSCS	
$\bar{\mu}$	p	λ_{nl}	λ_{nl}/λ_l	λ_{nl}	λ_{nl}/λ_l	λ_{nl}	λ_{nl}/λ_l
0	0	0.3122	1.0022	0.5290	1.0037	0.4337	1.0027
	1	0.2328	1.0055	0.4317	1.0061	0.3461	1.0051
	2	0.2019	1.0067	0.4014	1.0066	0.3170	1.0055
	3	0.1813	1.0076	0.3837	1.0067	0.2993	1.0057
	4	0.1652	1.0084	0.3708	1.0068	0.2863	1.0059
	5	0.1516	1.0094	0.3605	1.0069	0.2758	1.0060
0.4	0	0.3091	1.0022	0.5229	1.0037	0.4290	1.0027
	1	0.2306	1.0055	0.4266	1.0062	0.3424	1.0051
	2	0.1999	1.0067	0.3967	1.0066	0.3136	1.0055
	3	0.1796	1.0076	0.3792	1.0067	0.2961	1.0057
	4	0.1636	1.0084	0.3664	1.0068	0.2832	1.0059
	5	0.1502	1.0094	0.3563	1.0069	0.2728	1.0060
0.8	0	0.3062	1.0022	0.5169	1.0038	0.4245	1.0027
	1	0.2284	1.0055	0.4218	1.0062	0.3388	1.0051
	2	0.1980	1.0067	0.3922	1.0066	0.3103	1.0055
	3	0.1779	1.0076	0.3748	1.0068	0.2930	1.0058
	4	0.1620	1.0084	0.3622	1.0068	0.2802	1.0059
	5	0.1487	1.0094	0.3522	1.0069	0.2699	1.0060
1.2	0	0.3033	1.0022	0.5111	1.0038	0.4202	1.0027
	1	0.2262	1.0055	0.4170	1.0062	0.3353	1.0051
	2	0.1962	1.0067	0.3878	1.0066	0.3071	1.0056
	3	0.1762	1.0076	0.3706	1.0068	0.2900	1.0058
	4	0.1605	1.0084	0.3581	1.0069	0.2773	1.0059
	5	0.1473	1.0094	0.3482	1.0070	0.2671	1.0060
1.6	0	0.3005	1.0022	0.5055	1.0038	0.4159	1.0027
	1	0.2241	1.0055	0.4125	1.0063	0.3319	1.0051
	2	0.1944	1.0067	0.3835	1.0067	0.3040	1.0056
	3	0.1746	1.0076	0.3665	1.0068	0.2870	1.0058
	4	0.1591	1.0084	0.3542	1.0069	0.2745	1.0059
	5	0.1460	1.0094	0.3444	1.0070	0.2644	1.0060
2	0	0.2978	1.0022	0.5001	1.0038	0.4118	1.0028
	1	0.2221	1.0055	0.4080	1.0063	0.3286	1.0051
	2	0.2978	1.0022	0.5001	1.0038	0.3009	1.0056
	3	0.2221	1.0055	0.4080	1.0063	0.2842	1.0058
	4	0.1926	1.0067	0.3794	1.0067	0.2718	1.0059
	5	0.1730	1.0076	0.3626	1.0068	0.2618	1.0061

(c) Two opposite edges clamped and the other edges movable simply-supported (CSCS)

$$U_0 = V_0 = W_0 = \Phi_X = \Phi_Y = \frac{\partial W_0}{\partial X} = 0 \qquad at\ edges\ X = 0,1$$
$$U_0 = W_0 = \Phi_X = \widehat{N}_{YY} = \widehat{M}_{YY} = \widehat{P}_{YY} = 0 \qquad at\ edges\ Y = 0,1 \tag{7}$$

4. Solution and numerical result

As an efficient approach, the DQ method (Shu 2012) along with iterative method (Ebrahimi and Hosseini 2016b, Malekzadeh 2007) are used to study the effect of nonlocal parameter $\bar{\mu}$, surface parameters, elastic foundation parameters and volume fraction exponent p, on nonlinear free vibrational behavior of FG nano-plates in hygrothermal environment for each of three cases of boundary conditions expressed in Eqs. (5)-(7).

It is supposed that the nano-FG plate has the ceramic (Silicon) at the heated surface $(z = h/2)$ and the metal (Al) at the cooled surface $(z = -h/2)$, and their compositions change as the power-law (Eq. (1)) function continuously in the thickness direction of the nano-plate. The temperature dependent material properties are taken into consideration as given in Table 1 from Refs. (Aluminum Association 1984, Mondolfo 2013, Poirier and Geiger 2016, Hull 1999). Under all boundary conditions, the nano-plate is subjected to a thermal loading, where the lower surface is held at $T_m = T_0 = 300\ K$ $(\Delta T_m = 0)$, and the upper surface experiences a temperature rise of ΔT_c from $T_0 = 300\ K$; meanwhile, the temperature rise in other points are nonlinear as depicted in Eq. (24.1).

For all boundary conditions we neglect the moisture absorption for metal

4.1 Convergence studying

In Fig. 2, the dimensionless frequency $\left(\lambda = \omega a \sqrt{\frac{\rho_c(T_0,h/2)}{E_c(T_0,h/2)}}\right)$ versus the number of grid points is plotted for two cases. Assuming surface parameters as Table 1 the curve (a) features the worst convergence situation while the curve (b) depicts the best convergence situation. Comparing these figures verifies that 30×30 grid points can approximate the final results with a good accuracy; therefore, all the results presented herein have been obtained using 30×30 mesh size.

4.2 Numerical results

Fig. 3, illustrates the variation of non-dimensional fundamental natural frequencies of Al/Si square FG nano-plates versus the volume fraction exponent for different dimensionless nonlocal parameter and three combinations of boundary conditions where $\Delta T_c = 450K$, $\Delta C = C_c - C_m = C_c = C_m = 0$ and surface parameters are the same as Table 1. As it is obvious when nonlocal parameter and volume fraction exponent increase the nonlinear frequency of the nano-plate decreases; the CCCC boundary condition appropriates higher value of frequency against other boundary conditions. The published numerical values are available in Table 2.

Fig. 4 demonstrates the effect of surface elastic modulus differential (ΔE_0) on nonlinear dimensionless fundamental frequencies of square FG nano -plate with different kinds of boundary conditions in thermal environment. The surface elastic modulus and surface elastic modulus differential (ΔE_0) are defined as

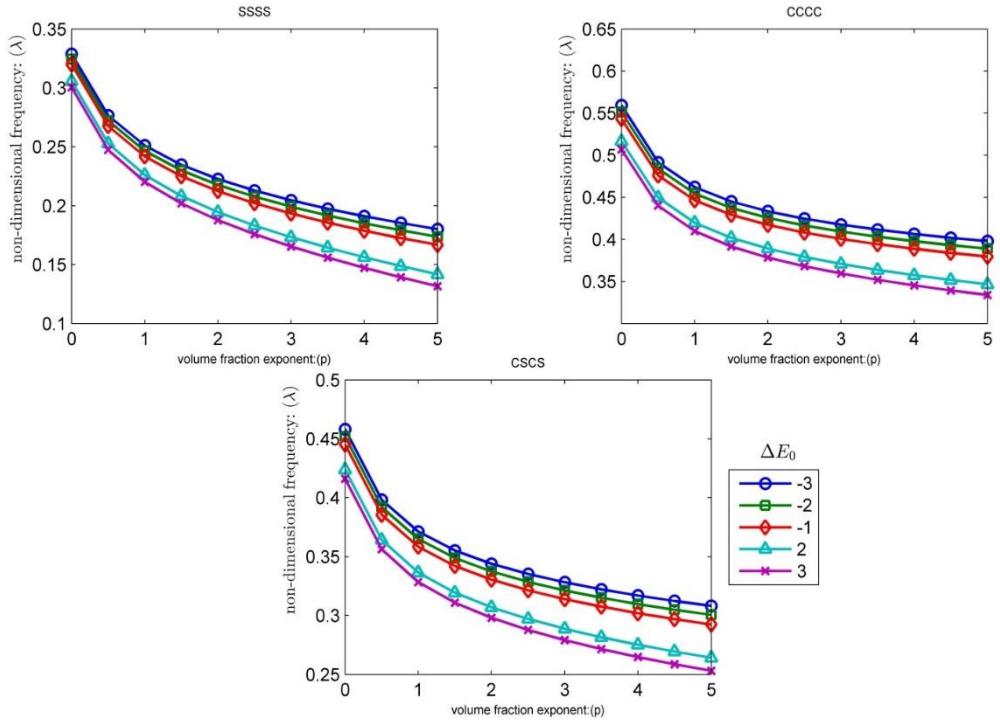

Fig. 4 Influence of surface elastic modulus differential on non-dimensional fundamental natural frequencies of square ($\boldsymbol{Al/Si}$) FG Reddy nano-plate with respect to various volume fraction exponent for different boundary conditions, considering surface stresses effect ($\boldsymbol{\bar{K}_w = \bar{K}_p = 0, h/a = 0.05, \bar{\mu} = 0.2, a = 200\ nm, \Delta T_c = 450\ K, \Delta C = C_c = 0}$)

Table 3 Influence of surface elastic modulus differential on non -dimensional fundamental natural frequencies of square (Al/Si) FG Reddy nano -plate with respect to various volume fraction exponent for different boundary conditions, considering surface stresses effect ($\bar{K}_w = \bar{K}_p = 0, h/a = 0.05, \bar{\mu} = 0.2, a = 200\ nm, \Delta T_c = 450\ K, \Delta C = C_c = 0$)

		SSSS		CCCC		CSCS	
$\frac{\Delta E_0}{E_{01}^{+} - E_{01}^{-}} = \frac{E_0^{+} - E_0^{-}}{E_{01}^{+} - E_{01}^{-}}$	p	λ_{nl}	λ_{nl}/λ_l	λ_{nl}	λ_{nl}/λ_l	λ_{nl}	λ_{nl}/λ_l
-3	0	0.4582	1.0019	0.5593	1.0028	0.4582	1.0019
	1	0.3712	1.0039	0.4620	1.0049	0.3712	1.0039
	2	0.3439	1.0042	0.4334	1.0052	0.3439	1.0042
	3	0.3282	1.0042	0.4175	1.0052	0.3282	1.0042
	4	0.3170	1.0043	0.4064	1.0052	0.3170	1.0043
	5	0.3082	1.0043	0.3978	1.0052	0.3082	1.0043
-2	0	0.4518	1.0021	0.5515	1.0030	0.4518	1.0021
	1	0.3650	1.0041	0.4544	1.0052	0.3650	1.0041
	2	0.3374	1.0045	0.4255	1.0055	0.3374	1.0045
	3	0.3213	1.0045	0.4093	1.0055	0.3213	1.0045
	4	0.3097	1.0046	0.3979	1.0055	0.3097	1.0046
	5	0.3006	1.0046	0.3889	1.0055	0.3006	1.0046
-1	0	0.4453	1.0023	0.5433	1.0032	0.4453	1.0023
	1	0.3584	1.0044	0.4464	1.0055	0.3584	1.0044
	2	0.3304	1.0048	0.4172	1.0058	0.3304	1.0048
	3	0.3139	1.0049	0.4006	1.0059	0.3139	1.0049
	4	0.3019	1.0049	0.3887	1.0059	0.3019	1.0049
	5	0.2924	1.0050	0.3795	1.0059	0.2924	1.0050
2	0	0.4239	1.0030	0.5166	1.0040	0.4239	1.0030
	1	0.3365	1.0055	0.4198	1.0066	0.3365	1.0055
	2	0.3069	1.0060	0.3891	1.0071	0.3069	1.0060
	3	0.2887	1.0063	0.3708	1.0073	0.2887	1.0063
	4	0.2751	1.0065	0.3574	1.0074	0.2751	1.0065
	5	0.2641	1.0067	0.3466	1.0075	0.2641	1.0067
3	0	0.4161	1.0033	0.5069	1.0044	0.4161	1.0033
	1	0.3283	1.0059	0.4098	1.0071	0.3283	1.0059
	2	0.2980	1.0066	0.3784	1.0076	0.2980	1.0066
	3	0.2791	1.0069	0.3595	1.0079	0.2791	1.0069
	4	0.2647	1.0072	0.3453	1.0081	0.2647	1.0072
	5	0.2530	1.0075	0.3339	1.0083	0.2530	1.0075

$$E_0 = 2\mu_0 + \lambda_0 \tag{50}$$

$$\Delta E_0 = \frac{E_0^{+} - E_0^{-}}{E_{01}^{+} - E_{01}^{-}} \tag{51}$$

where superscripts "+" and "-" denote upper and lower surface of the nano-plate and subscript "1" is related to primary values (Table 1) of surface parameters. The surface tension (τ_0) is considered temperature dependent. It is observed that an increase in ΔE_0 reduces the dimensionless fundamental frequency; it can also be seen with the increase in volume fraction exponent the constant elastic modulus differential curves ($\Delta E_0 = const$) diverge from each other which means by increasing the volume fraction exponent the effect of surface stresses enhances; in addition, the frequency

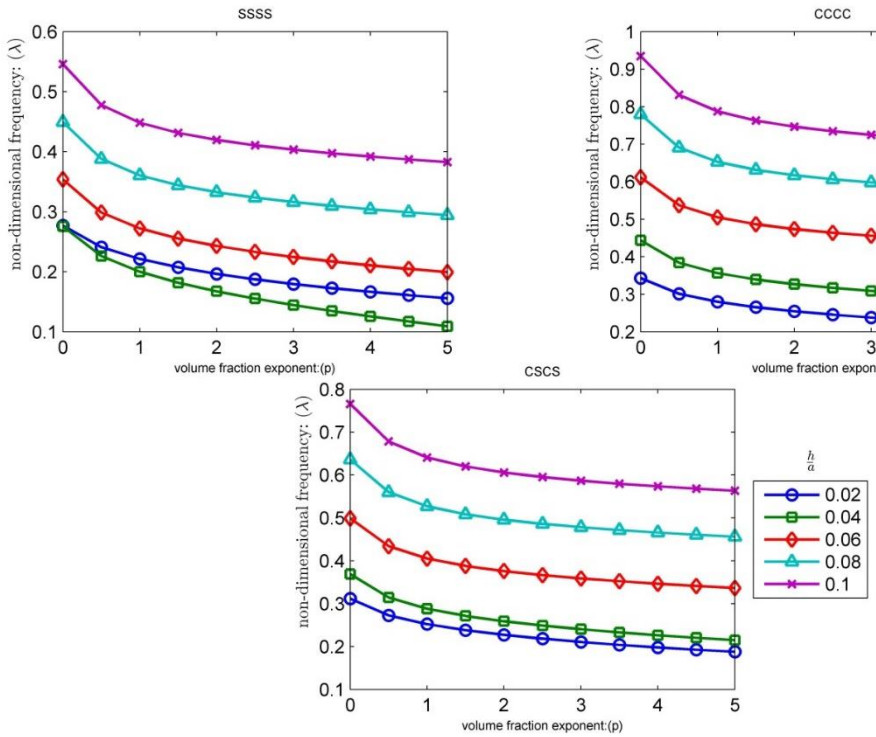

Fig. 5 Influence of non-dimensional thickness on non-dimensional fundamental natural frequencies of square $(\boldsymbol{Al/Si})$ FG Reddy nano-plate with respect to various volume fraction exponent for different boundary conditions, considering surface stresses effect $(\boldsymbol{\bar{K}_w = \bar{K}_p = 0, \bar{\mu} = 0.2, a = 200\ nm, \Delta T_c = 450\ K, \Delta C = C_c = 0})$

Table 4 Influence of non-dimensional thickness on non-dimensional fundamental natural frequencies of square (Al/Si) FG Reddy nano -plate with respect to various volume fraction exponent for different boundary conditions, considering surface stresses effect $(\bar{K}_w = \bar{K}_p = 0, \bar{\mu} = 0.2, a = 200\ nm, \Delta T_c = 450\ K, \Delta C = C_c = 0)$

		SSSS		CCCC		CSCS	
h/a	p	λ_{nl}	λ_{nl}/λ_l	λ_{nl}	λ_{nl}/λ_l	λ_{nl}	λ_{nl}/λ_l
0.02	0	0.3116	1.0010	0.3430	1.0015	0.3116	1.0010
	1	0.2522	1.0017	0.2800	1.0024	0.2522	1.0017
	2	0.2273	1.0019	0.2546	1.0027	0.2273	1.0019
	3	0.2106	1.0021	0.2380	1.0029	0.2106	1.0021
	4	0.1980	1.0023	0.2254	1.0032	0.1980	1.0023
	5	0.1877	1.0024	0.2153	1.0034	0.1877	1.0024
0.04	0	0.3689	1.0025	0.4438	1.0035	0.3689	1.0025
	1	0.2883	1.0049	0.3563	1.0060	0.2883	1.0049
	2	0.2590	1.0056	0.3269	1.0066	0.2590	1.0056
	3	0.2404	1.0060	0.3089	1.0070	0.2404	1.0060
	4	0.2263	1.0064	0.2955	1.0072	0.2263	1.0064
	5	0.2149	1.0067	0.2848	1.0075	0.2149	1.0067
0.06	0	0.4992	1.0027	0.6117	1.0038	0.4992	1.0027
	1	0.4052	1.0050	0.5052	1.0061	0.4052	1.0050
	2	0.3760	1.0053	0.4738	1.0063	0.3760	1.0053
	3	0.3589	1.0053	0.4560	1.0064	0.3589	1.0053
	4	0.3465	1.0054	0.4432	1.0064	0.3465	1.0054
	5	0.3366	1.0054	0.4331	1.0064	0.3366	1.0054
0.08	0	0.6363	1.0026	0.7798	1.0037	0.6363	1.0026
	1	0.5273	1.0047	0.6530	1.0058	0.5273	1.0047
	2	0.4957	1.0048	0.6173	1.0059	0.4957	1.0048
	3	0.4782	1.0048	0.5979	1.0058	0.4782	1.0048
	4	0.4657	1.0047	0.5844	1.0057	0.4657	1.0047
	5	0.4560	1.0046	0.5739	1.0057	0.4560	1.0046
0.1	0	0.7659	1.0025	0.9348	1.0036	0.7659	1.0025
	1	0.6410	1.0045	0.7876	1.0056	0.6410	1.0045
	2	0.6059	1.0046	0.7466	1.0057	0.6059	1.0046
	3	0.5868	1.0044	0.7248	1.0056	0.5868	1.0044
	4	0.5736	1.0043	0.7099	1.0054	0.5736	1.0043
	5	0.5635	1.0042	0.6986	1.0053	0.5635	1.0042

curves in CCCC and SSSS FG nano-plates are higher and lower, respectively, than that for CSCS nano-plate. The numerical result for this case can be found in Table 3.

Fig. 5 features the influence of the dimensionless thickness on the frequency response of the FG nano-plate with different volume fraction exponent and boundary condition in thermal environment. As the mentioned figure shows, by enlarging the thickness, dimensionless frequency will increase; the rate of this increasing is faster in CCCC boundary condition than those for other types of boundary condition. The coincident numerical results for this case have been listed in Table 4.

Dimensionless fundamental frequency variation of the FG

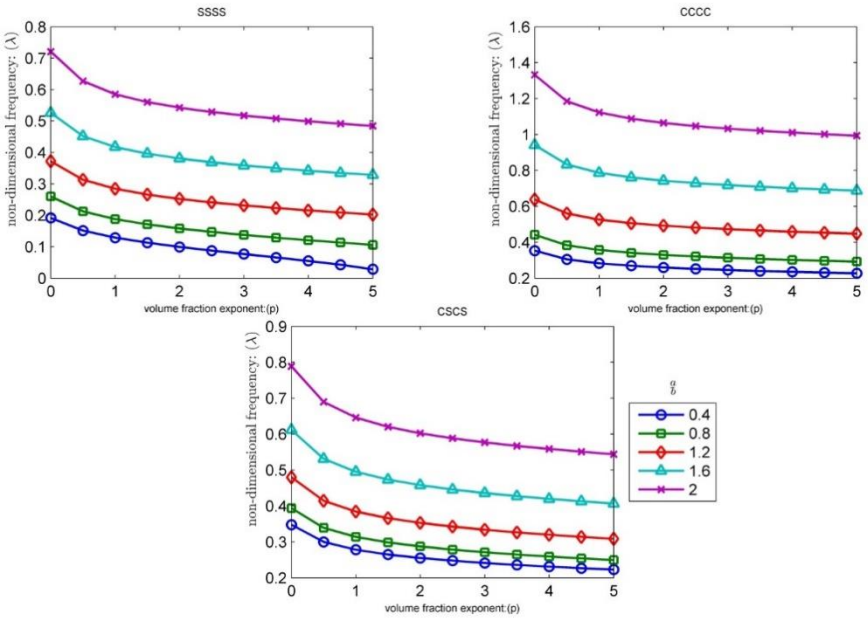

Fig. 6 Influence of aspect ratio on non-dimensional fundamental natural frequencies of $(\boldsymbol{Al/Si})$ FG Reddy nano -plate with respect to various volume fraction exponent for different boundary conditions, considering surface stresses effect $(\boldsymbol{\bar{K}_w = \bar{K}_p = 0, h/a = 0.05, \bar{\mu} = 0.2, a = 200\ nm, \Delta T_c = 450\ K, \Delta C = C_c = 0})$

Table 5 Influence of aspect ratio on non -dimensional fundamental natural frequencies of (Al/Si) FG Reddy nano-plate with respect to various volume fraction exponent for different boundary conditions, considering surface stresses effect $(\bar{K}_w = \bar{K}_p = 0, h/a = 0.05, \bar{\mu} = 0.2, a = 200\ nm, \Delta T_c = 450\ K, \Delta C = C_c = 0)$

		SSSS		CCCC		CSCS	
a/b	p	λ_{nl}	λ_{nl}/λ_l	λ_{nl}	λ_{nl}/λ_l	λ_{nl}	λ_{nl}/λ_l
0.4	0	0.3480	1.0030	0.3533	1.0035	0.3480	1.0030
	1	0.2781	1.0040	0.2827	1.0049	0.2781	1.0040
	2	0.2551	1.0044	0.2596	1.0053	0.2551	1.0044
	3	0.2412	1.0046	0.2457	1.0056	0.2412	1.0046
	4	0.2310	1.0048	0.2354	1.0059	0.2310	1.0048
	5	0.2227	1.0050	0.2271	1.0061	0.2227	1.0050
0.8	0	0.3937	1.0029	0.4419	1.0037	0.3937	1.0029
	1	0.3138	1.0049	0.3570	1.0061	0.3138	1.0049
	2	0.2872	1.0053	0.3298	1.0066	0.2872	1.0053
	3	0.2711	1.0055	0.3136	1.0068	0.2711	1.0055
	4	0.2591	1.0057	0.3017	1.0070	0.2591	1.0057
	5	0.2495	1.0059	0.2922	1.0072	0.2495	1.0059
1.2	0	0.4799	1.0025	0.6383	1.0038	0.4799	1.0025
	1	0.3843	1.0050	0.5261	1.0060	0.3843	1.0050
	2	0.3528	1.0055	0.4923	1.0063	0.3528	1.0055
	3	0.3338	1.0056	0.4729	1.0063	0.3338	1.0056
	4	0.3197	1.0057	0.4589	1.0064	0.3197	1.0057
	5	0.3085	1.0058	0.4479	1.0064	0.3085	1.0058
1.6	0	0.6116	1.0020	0.9411	1.0037	0.6116	1.0020
	1	0.4951	1.0044	0.7870	1.0054	0.4951	1.0044
	2	0.4579	1.0047	0.7430	1.0055	0.4579	1.0047
	3	0.4359	1.0047	0.7185	1.0055	0.4359	1.0047
	4	0.4197	1.0047	0.7013	1.0054	0.4197	1.0047
	5	0.4068	1.0047	0.6878	1.0054	0.4068	1.0047
2	0	0.7888	1.0014	1.3325	1.0037	0.7888	1.0014
	1	0.6461	1.0034	1.1230	1.0049	0.6461	1.0034
	2	0.6023	1.0036	1.0644	1.0050	0.6023	1.0036
	3	0.5770	1.0036	1.0327	1.0049	0.5770	1.0036
	4	0.5585	1.0035	1.0107	1.0049	0.5585	1.0035
	5	0.5439	1.0035	0.9938	1.0048	0.5439	1.0035

nano-plate is presented in Fig. 6 for various values of aspect ratio and volume fraction exponent in thermal environment and under different boundary conditions. It can be found that the dimensionless fundamental frequency increases by the increase in aspect ratio. Among different boundary conditions the highest values of dimensionless frequency belong to CCCC boundary condition. The numerical results for this case have been listed in Table 5.

Fig. 7, display the variation of non -dimensional fundamental frequency of square FG nano-plate with respect to the volume fraction exponent resting on Winkler-Pasternak foundation, respectively. It can be observed that the influence of shear modulus on dimensionless frequencies of FG nano-plate is more significant than Winkler parameters. Fig. 7, illustrate that for a FG nano-plate lying on elastic foundations with the same shear modulus, variation of Winkler modulus has low effect on dimensionless frequency variation. The dimensionless fundamental frequency tends to higher values

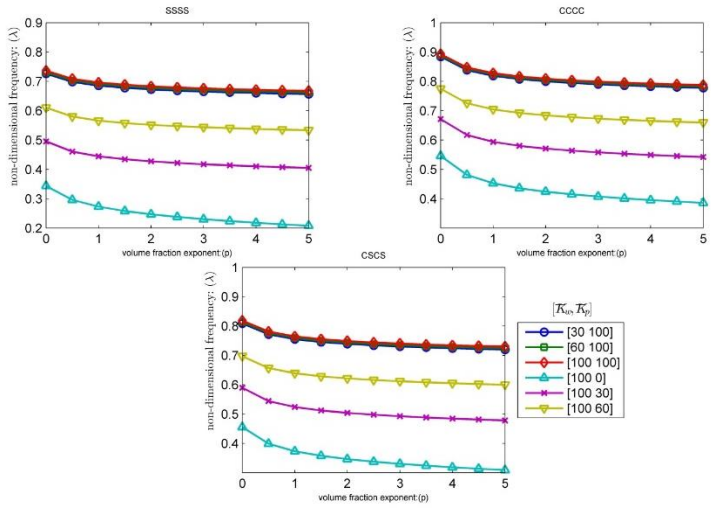

Fig. 7 Influence of Pasternak and Winkler parameters on non -dimensional fundamental natural frequencies of square ($\boldsymbol{Al/Si}$) FG Reddy nano-plate with respect to various volume fraction exponent for different boundary conditions, considering surface stresses effect ($\boldsymbol{h/a = 0.05, \bar{\mu} = 0.2, a = 200\,nm, \Delta T_c = 450\,K, \Delta C = C_c = 0}$)

Table 6 Influence of Pasternak and Winkler parameters on non-dimensional fundamental natural frequencies of square ($\boldsymbol{Al/Si}$) FG Reddy nano -plate with respect to various volume fraction exponent for different boundary conditions, considering surface stresses effect ($\boldsymbol{h/a = 0.05, \bar{\mu} = 0.2, a = 200\,nm, \Delta T_c = 450\,K, \Delta C = C_c = 0}$)

			SSSS		CCCC		CSCS	
$\bar{K}_w$	$\bar{K}_p$	p	λ_{nl}	λ_{nl}/λ_l	λ_{nl}	λ_{nl}/λ_l	λ_{nl}	λ_{nl}/λ_l
100	0	0	0.7365	1.0004	0.8929	1.0011	0.8183	1.0006
		1	0.6961	1.0006	0.8279	1.0013	0.7648	1.0009
		2	0.6833	1.0006	0.8092	1.0012	0.7488	1.0009
		3	0.6761	1.0006	0.7992	1.0012	0.7401	1.0008
		4	0.6712	1.0005	0.7923	1.0011	0.7342	1.0008
		5	0.6675	1.0005	0.7872	1.0011	0.7297	1.0007
100	30	0	0.3435	1.0018	0.5460	1.0035	0.4556	1.0024
		1	0.2729	1.0039	0.4527	1.0055	0.3732	1.0043
		2	0.2468	1.0044	0.4240	1.0058	0.3463	1.0046
		3	0.2303	1.0046	0.4074	1.0059	0.3303	1.0047
		4	0.2178	1.0048	0.3953	1.0059	0.3186	1.0047
		5	0.2077	1.0049	0.3858	1.0060	0.3092	1.0047
100	60	0	0.4953	1.0008	0.6713	1.0021	0.5896	1.0014
		1	0.4444	1.0015	0.5937	1.0029	0.5241	1.0021
		2	0.4274	1.0015	0.5708	1.0029	0.5040	1.0020
		3	0.4174	1.0014	0.5581	1.0028	0.4926	1.0019
		4	0.4103	1.0014	0.5491	1.0027	0.4845	1.0019
		5	0.4048	1.0013	0.5422	1.0026	0.4782	1.0018
100	100	0	0.6104	1.0005	0.7749	1.0015	0.6973	1.0009
		1	0.5662	1.0009	0.7046	1.0019	0.6390	1.0013
		2	0.5518	1.0009	0.6843	1.0019	0.6214	1.0013
		3	0.5436	1.0009	0.6731	1.0018	0.6117	1.0012
		4	0.5378	1.0008	0.6654	1.0017	0.6049	1.0011
		5	0.5335	1.0008	0.6596	1.0016	0.5997	1.0011

Table 7 Influence of thermal loading on non-dimensional fundamental natural frequencies of square (Al/Si) FG Reddy nano -plate with respect to various volume fraction exponent for different boundary conditions, considering surface stresses effect ($\bar{K}_w = \bar{K}_p = 0, h/a = 0.05, \bar{\mu} = 0.2, a = 200\,nm,\ \Delta C = C_c = 0$)

		SSSS		CCCC		CSCS	
$\Delta T_c\ (K)$	p	λ_{nl}	λ_{nl}/λ_l	λ_{nl}	λ_{nl}/λ_l	λ_{nl}	λ_{nl}/λ_l
300	0	0.4410	1.0026	0.5355	1.0036	0.4410	1.0026
	1	0.3649	1.0045	0.4483	1.0057	0.3649	1.0045
	2	0.3419	1.0047	0.4233	1.0058	0.3419	1.0047
	3	0.3288	1.0047	0.4095	1.0058	0.3288	1.0047
	4	0.3196	1.0047	0.3998	1.0058	0.3196	1.0047
	5	0.3124	1.0047	0.3923	1.0057	0.3124	1.0047
450	0	0.4313	1.0027	0.5259	1.0037	0.4313	1.0027
	1	0.3442	1.0051	0.4292	1.0062	0.3442	1.0051
	2	0.3153	1.0055	0.3990	1.0066	0.3153	1.0055
	3	0.2977	1.0057	0.3814	1.0067	0.2977	1.0057
	4	0.2847	1.0059	0.3686	1.0068	0.2847	1.0059
	5	0.2743	1.0060	0.3584	1.0069	0.2743	1.0060
600	0	0.4217	1.0028	0.5164	1.0038	0.4217	1.0028
	1	0.3235	1.0057	0.4102	1.0067	0.3235	1.0057
	2	0.2883	1.0066	0.3749	1.0075	0.2883	1.0066
	3	0.2655	1.0072	0.3531	1.0079	0.2655	1.0072
	4	0.2479	1.0077	0.3367	1.0082	0.2479	1.0077
	5	0.2331	1.0083	0.3232	1.0085	0.2331	1.0083

when shear modulus of foundation increases. The numerical results for this figure are tabulated in Table 6.

Fig. 8 features the role of thermal loading in variation of dimensionless frequency of the FG nano-plate. As it is clear from this figure, thermal loading has a contrary effect on dimensionless frequency of Al/Si FG nao-plate, which in the

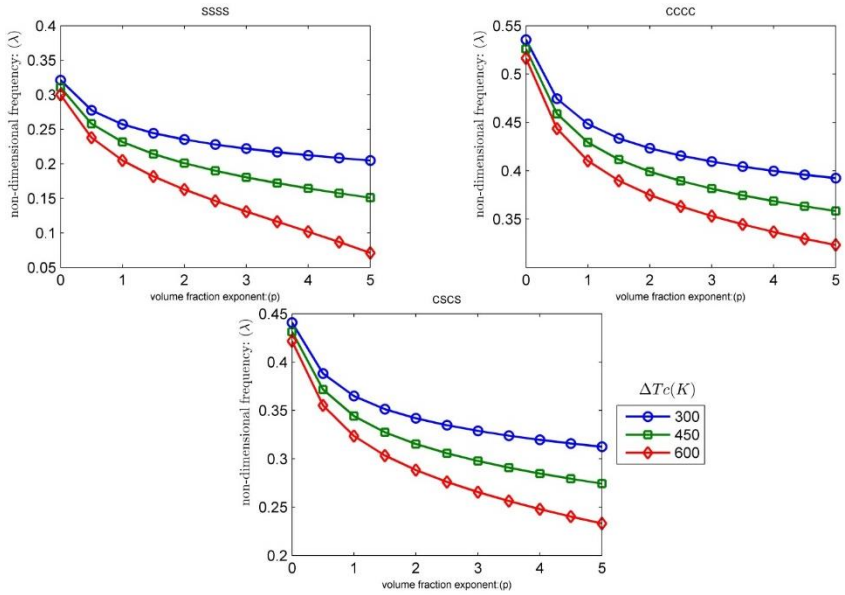

Fig. 8 Influence of thermal loading on non -dimensional fundamental natural frequencies of square $(\boldsymbol{Al/Si})$ FG Reddy nano-plate with respect to various volume fraction exponent for different boundary conditions, considering surface stresses effect $(\bar{\boldsymbol{K}}_{\boldsymbol{w}} = \bar{\boldsymbol{K}}_{\boldsymbol{p}} = \boldsymbol{0}, \boldsymbol{h/a} = \boldsymbol{0.05}, \bar{\boldsymbol{\mu}} = \boldsymbol{0.2}, \boldsymbol{a} = \boldsymbol{200\ nm}, \boldsymbol{\Delta C} = \boldsymbol{C_c} = \boldsymbol{0})$

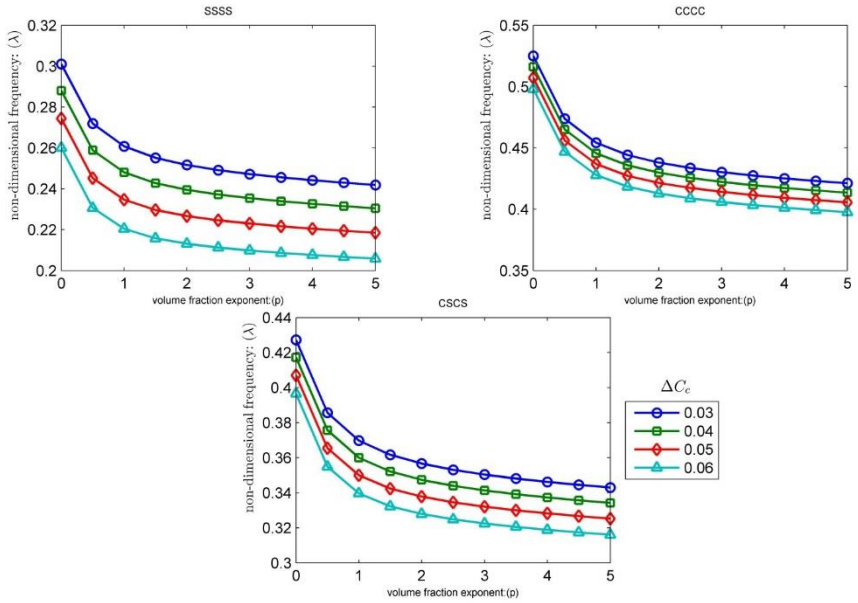

Fig. 9 Influence of moisture concentration variation on non-dimensional fundamental natural frequencies of square $(\boldsymbol{Al/Si})$ FG Reddy nano-plate with respect to various volume fraction exponent for different boundary conditions, considering surface stresses effect $(\bar{\boldsymbol{K}}_{\boldsymbol{w}} = \bar{\boldsymbol{K}}_{\boldsymbol{p}} = \boldsymbol{0}, \boldsymbol{h/a} = \boldsymbol{0.05}, \bar{\boldsymbol{\mu}} = \boldsymbol{0.2}, \boldsymbol{a} = \boldsymbol{200\ nm}, \boldsymbol{\Delta T_c} = \boldsymbol{70\ K})$

result the increasing of temperature yields the decreasing of dimensionless frequency. Like other cases, the higher values of dimensionless frequency belong in CCCC boundary condition. The listed numerical results are available in Table 7.

In Fig. 9, dimensionless fundamental frequencies are plotted versus the volume fraction exponent for different moisture concentration variation and different boundary conditions. From this figure, it is clearly seen that similar to thermal loading, moisture concentration variation has a reverse effect on the dimensionless frequencies and higher moisture concentration causes lower dimensionless frequencies. CCCC boundary condition still possesses higher value of dimensionless frequencies. The numerical results are listed in Table 8.

Knowing that the maximum melting point of Al is $933.4^{\circ}K$ (Mondolfo 2013), Table 9 gives the nondimensionalized values of fundamental natural frequencies for various boundary conditions and Pasternak modulus (since Winkler modulus has miserly effect on frequencies we just consider the change of Pasternak modulus); it can be observed that as long as Pasternak

Table 8 Influence of moisture concentration variation on non -dimensional fundamental natural frequencies of square ($\boldsymbol{Al/Si}$) FG Reddy nano -plate with respect to various volume fraction exponent for different boundary conditions, considering surface stresses effect ($\boldsymbol{\bar{K}_w = \bar{K}_p = 0, h/a = 0.05, \bar{\mu} = 0.2, a = 200\ nm, \Delta T_c = 70\ K}$)

		SSSS		CCCC		CSCS	
$\Delta C_c = C_c$	p	λ_{nl}	λ_{nl}/λ_l	λ_{nl}	λ_{nl}/λ_l	λ_{nl}	λ_{nl}/λ_l
0.03	0	0.3010	1.0024	0.5250	1.0039	0.4273	1.0029
	1	0.2608	1.0045	0.4542	1.0057	0.3698	1.0045
	2	0.2517	1.0044	0.4381	1.0056	0.3567	1.0045
	3	0.2472	1.0042	0.4303	1.0054	0.3504	1.0043
	4	0.2442	1.0040	0.4251	1.0052	0.3462	1.0041
	5	0.2419	1.0038	0.4212	1.0051	0.3430	1.0040
0.04	0	0.2880	1.0026	0.5162	1.0041	0.4173	1.0031
	1	0.2481	1.0049	0.4456	1.0059	0.3600	1.0048
	2	0.2395	1.0049	0.4298	1.0058	0.3474	1.0047
	3	0.2354	1.0046	0.4223	1.0056	0.3413	1.0045
	4	0.2327	1.0044	0.4173	1.0054	0.3373	1.0043
	5	0.2305	1.0042	0.4135	1.0053	0.3342	1.0042
0.05	0	0.2744	1.0029	0.5072	1.0042	0.4071	1.0032
	1	0.2347	1.0055	0.4369	1.0062	0.3500	1.0051
	2	0.2267	1.0054	0.4215	1.0061	0.3378	1.0050
	3	0.2230	1.0052	0.4142	1.0059	0.3320	1.0048
	4	0.2205	1.0049	0.4094	1.0057	0.3282	1.0046
	5	0.2185	1.0047	0.4057	1.0055	0.3253	1.0044
0.06	0	0.2601	1.0032	0.4981	1.0044	0.3966	1.0034
	1	0.2205	1.0063	0.4279	1.0065	0.3397	1.0054
	2	0.2131	1.0062	0.4129	1.0064	0.3279	1.0053
	3	0.2098	1.0058	0.4059	1.0062	0.3225	1.0051
	4	0.2076	1.0055	0.4012	1.0060	0.3189	1.0049
	5	0.2058	1.0053	0.3977	1.0058	0.3160	1.0047

modulus is zero, the effect of nonlocal parameter, for each thermal loading is decreasing, meaning, by increasing the value of nonlocal parameter, the amount of natural frequencies are reduced. For non-zero values of Pasternak modulus, the effect of nonlocal parameters on natural frequencies is related to support configuration. When support configuration comprises clamp types the effect of nonlocal parameters, for each thermal loading will be increasing, while for SSSS configuration the effect of nonlocal parameter is decreasing. Comparing the values shows that the amount of nonlocal parameter has no effect on the natural effect of thermal loading or Pasternak parameter on non-dimensional natural frequencies; so, we can conclude that for every value of nonlocal parameter, thermal loading and Pasternak parameter has decreasing and increasing effect, respectively, on non-dimensional natural frequencies.

4.3 Verification of the results

To verify the present approach, the numerical results of

Table 9 Influence of nonlocal parameter on non – dimensional fundamental natural frequencies of square ($\boldsymbol{Al/Si}$) FG Reddy nano -plate with respect to various thermal loading, foundation parameters and boundary conditions, considering surface stresses effect ($\boldsymbol{h/a = 0.05, a = 200\ nm, \Delta C = C_c = 0}$)

			SSSS		CCCC		CSCS	
$(\bar{K}_w, \bar{K}_p)$	$\Delta T_c\ (K)$	$\bar{\mu}$	λ_{nl}	λ_{nl}/λ_l	λ_{nl}	λ_{nl}/λ_l	λ_{nl}	λ_{nl}/λ_l
(100,0)	300	0.4	0.2632	1.0036	0.4315	1.0052	0.3570	1.0040
		1.2	0.2598	1.0035	0.4229	1.0052	0.3508	1.0040
		2	0.2565	1.0035	0.4148	1.0052	0.3450	1.0039
	450	0.4	0.2296	1.0046	0.4053	1.0059	0.3289	1.0047
		1.2	0.2270	1.0045	0.3973	1.0059	0.3233	1.0046
		2	0.2245	1.0045	0.3898	1.0059	0.3182	1.0046
	600	0.4	0.1935	1.0064	0.3791	1.0067	0.3004	1.0056
		1.2	0.1919	1.0063	0.3717	1.0067	0.2955	1.0055
		2	0.1903	1.0061	0.3648	1.0068	0.2910	1.0055
(100,30)	300	0.4	0.4365	1.0013	0.5776	1.0026	0.5117	1.0018
		1.2	0.4344	1.0013	0.5792	1.0025	0.5119	1.0018
		2	0.4324	1.0013	0.5804	1.0025	0.5120	1.0017
	450	0.4	0.4170	1.0014	0.5588	1.0027	0.4928	1.0019
		1.2	0.4156	1.0014	0.5611	1.0027	0.4938	1.0019
		2	0.4143	1.0013	0.5631	1.0026	0.4945	1.0018
	600	0.4	0.3984	1.0015	0.5407	1.0029	0.4747	1.0021
		1.2	0.3976	1.0015	0.5439	1.0028	0.4764	1.0020
		2	0.3969	1.0014	0.5466	1.0027	0.4778	1.0019
(100,60)	300	0.4	0.5583	1.0008	0.6913	1.0017	0.6282	1.0012
		1.2	0.5567	1.0008	0.7000	1.0017	0.6325	1.0011
		2	0.5552	1.0008	0.7072	1.0016	0.6360	1.0011
	450	0.4	0.5433	1.0009	0.6759	1.0018	0.6131	1.0012
		1.2	0.5422	1.0008	0.6853	1.0017	0.6179	1.0012
		2	0.5411	1.0008	0.6932	1.0016	0.6221	1.0011
	600	0.4	0.5292	1.0009	0.6613	1.0018	0.5988	1.0012
		1.2	0.5286	1.0009	0.6715	1.0017	0.6043	1.0012
		2	0.5280	1.0008	0.6800	1.0017	0.6090	1.0012

clamped $ZrO_2/Ti-6Al-4V$ FG square plates are compared with those published in Ref. (Kim 2005) which consider a third order FGM plate in thermal environment; the effective temperature dependent material properties are modeled by the rule of mixture and power-law volume fraction distribution; the required temperature dependent material properties are available in Table 1. In addition to these assumptions, the nonlocal and surface parameters are set to zero. As it can be seen from Table 10, for nonlinear temperature rise, there is a good agreement between the present first 8 natural frequencies and those of aforesaid reference.

5. Conclusions

The surface effect on free vibration of FG rectangular

Table 10 Comparison of eight first non –dimensional natural frequencies ($\lambda = \omega b^2/\pi^2\sqrt{I_S/D_S}$)[7] of square ($Ti-6Al-4V/ZrO_2$) FG plate($\bar{K}_w = \bar{K}_p = 0, h/a = 0.1, \bar{\mu} = 0, a = 0.2m,\ \Delta T_c = 500\ K, \Delta T_m = 0\ K, \Delta C = 0, \rho_{0m} = \rho_{0c} = 0, \lambda_{0m} = \mu_{0m} = \tau_{0m} = \lambda_{0c} = \mu_{0c} = \tau_{0c} = 0$)

		Mode sequence							
p		1	2	3	4	5	6	7	8
0	Present	3.1436	6.1159	6.1159	8.6356	10.2090	10.3104	12.3845	12.3845
	Ref. (Kim 2005)	3.3704	6.5920	6.5920	9.3125	10.8924	10.9807	13.2730	13.2730
	Error (%)	6.7305	7.2222	7.2222	7.2684	6.2740	6.1045	6.6938	6.6938
0.2	Present	3.1773	6.1593	6.1593	8.6856	10.2619	10.3627	12.4423	12.4423
	Ref. (Kim 2005)	3.3040	6.4613	6.4613	9.1303	10.6833	10.7692	13.0201	13.0201
	Error (%)	3.8361	4.6743	4.6743	4.8711	3.9441	3.7748	4.4380	4.4380
1	Present	3.1864	6.1678	6.1678	8.6957	10.2752	10.3742	12.4588	12.4588
	Ref. (Kim 2005)	3.1584	6.1792	6.1792	8.7349	10.2239	10.3058	12.4627	12.4627
	Error (%)	0.8874	0.1842	0.1842	0.4482	0.5019	0.6642	0.0311	0.0311
5	Present	3.1646	6.1367	6.1367	8.6619	10.2438	10.3412	12.4289	12.4289
	Ref. (Kim 2005)	2.9970	5.8742	5.8742	8.3078	9.7238	9.8023	11.8553	11.8553
	Error (%)	5.5918	4.4679	4.4679	4.2618	5.3478	5.4973	4.8381	4.8381

nano-plate subjected to nonlinear temperature field is investigated in present study. The governing equations are obtained based on Reddy's plate theory and include geometric nonlinearity using von Karman's assumptions. The temperature dependent material properties are assumed to be varied through the thickness of the nano-plate based on Mori-Tanaka homogenization scheme. Using iterative and DQ methods the equations of motion are solved and the accuracy of the present approach is validated by comparing the present result and the result of other paper. Knowing that obtained governing equations are dimensionless, to set logical values for dimensionless parameters the properties of Al/Si FGM were used. From the results presented herein, the following observations can be made:

1. With the increase in nonlocal parameter and volume fraction exponent, the fundamental frequency of the FG nano-plate decreases.

2. Considering the residual surface stress (τ_0) dependency on temperature, the surface parameters have decreasing effect on the fundamental frequency of FG nano-plate.

3. The increase in volume fraction exponent, enhances the effect of surface stresses on the fundamental frequency of FG nano-plate.

4. With the increase in geometrical parameters (dimensionless thickness and aspect ratio), dimensionless frequency will increase.

5. The effect of Pasternak parameter on the natural frequency is significantly more than Winkler parameter's effect

6. Pasternak parameter increase for every value of nonlocal parameter has increasing effect on non-dimensional natural frequency.

7. Supporting of FG nano-plate with clamp boundary condition can enhance fundamental frequency.

8. Hygrothermal environment has decreasing effect on the fundamental frequency, meaning with the increase in temperature or moisture concentration, the fundamental frequency decreases.

9. Increasing the thermal load for every value of nonlocal parameter has decreasing effect on non-dimensional natural frequency.

[7] $I_s = \rho_m h$
$D_s = E_m h^3/12(1-\upsilon_m^2)$

References

Ahn, S.J. (2004), *Least Squares Orthogonal Distance Fitting of Curves and Surfaces in Space*, Springer Science & Business Media.

Ansari, R. and Gholami, R. (2016), "Surface effect on the large amplitude periodic forced vibration of first-order shear deformable rectangular nanoplates with various edge supports", *Acta Astronaut.*, **118**, 72-89.

Ansari, R., Ashrafi, M.A., Pourashraf, S. and Sahmani, S. (2015), "Vibration and buckling characteristics of functionally graded nanoplates subjected to thermal loading based on surface elasticity theory", *Acta Astronaut.*, **109**, 42-51.

Ansari, R., Faghih Shojaei, M., Mohammadi, V., Gholami, R. and Darabi, M.A. (2014), "Nonlinear vibrations of functionally graded Mindlin microplates based on the modified couple stress theory", *Compos. Struct.*, **114**, 124-134.

Ansari, R., Shojaei, M.F., Shahabodini, A. and Vahdati, M.B. (2015), "Three-dimensional bending and vibration analysis of functionally graded nanoplates by a novel differential quadrature-based approach", *Compos. Struct.*, **131**, 753-764.

Barati, M.R. and Shahverdi, H. (2016), "A four-variable plate theory for thermal vibration of embedded FG nanoplates under non-uniform temperature distributions with different boundary conditions", *Struct. Eng. Mech.*, **60**(4), 707-727.

Barati, M.R. and Shahverdi, H. (2017), "An analytical solution for thermal vibration of compositionally graded nanoplates with arbitrary boundary conditions based on physical neutral surface position", *Mech. Adv. Mater. Struct.*, **24**(10), 840-853.

Barati, M.R., Zenkour, A.M. and Shahverdi, H. (2016), "Thermo-mechanical buckling analysis of embedded nanosize FG plates in thermal environments via an inverse cotangential theory", *Compos. Struct.*, **141**, 203-212.

Berthelot, J.M. (2012), *Composite Materials: Mechanical Behavior and Structural Analysis*, Springer Science & Business Media.

Bloom, F. and Coffin, D.W. (2000), "Modelling the hygroscopic buckling of layered paper sheets", *Math. Comput. Modell.*, **31**(8-9), 43-60.

Chen, W.J. and Li, X.P. (2013), "Size-dependent free vibration analysis of composite laminated Timoshenko beam based on new modified couple stress theory", *Arch. Appl. Mech.*, **83**(3), 431-444.

Daneshmehr, A., Rauabpoor, A. and Hadi, A. (2015), "Size dependent free vibration analysis of nanoplates made of functionally graded materials based on nonlocal elasticity theory with high order theories", *Int. J. Eng. Sci.*, **95**, 23-35.

Draiche, K., Tounsi, A. and Mahmoud, S.R. (2016), "A refined

theory with stretching effect for the flexure analysis of laminated composite plates", *Geomech. Eng.*, **11**(5), 671-690.
Duffy, D.G. (2015), *Green's Functions with Applications*, CRC Press.
Ebrahimi, F. and Barati, M.R. (2016a), "Static stability analysis of smart magneto-electro-elastic heterogeneous nanoplates embedded in an elastic medium based on a four-variable refined plate theory", *Smart Mater. Struct.*, **25**(10), 105014.
Ebrahimi, F. and Barati, M.R. (2016b), "Size-dependent thermal stability analysis of graded piezomagnetic nanoplates on elastic medium subjected to various thermal environments", *Appl. Phys. A*, **122**(10), 910.
Ebrahimi, F. and Barati, M.R. (2016c), "Temperature distribution effects on buckling behavior of smart heterogeneous nanosize plates based on nonlocal four-variable refined plate theory", *Int. J. Nano Mater.*, **7**(3), 119-143.
Ebrahimi, F. and Barati, M.R. (2017a), "Investigating physical field effects on the size-dependent dynamic behavior of inhomogeneous nanoscale plates", *Eur. Phys. J. Plus*, **132**(2).
Ebrahimi, F. and Barati, M.R. (2017b), "Buckling analysis of piezoelectrically actuated smart nanoscale plates subjected to magnetic field", *J. Intellig. Mater. Syst. Struct.*, **28**(11), 1472-1490.
Ebrahimi, F. and Barati, M.R. (2017c), "Magnetic field effects on dynamic behavior of inhomogeneous thermo-piezo-electrically actuated nanoplates", *J. Brazil. Soc. Mech. Sci. Eng.*, **39**(6), 2203-2223.
Ebrahimi, F. and Barati, M.R. (2017d), "Damping vibration analysis of smart piezoelectric polymeric nanoplates on viscoelastic substrate based on nonlocal strain gradient theory", *Smart Mater. Struct.*, **26**(6), 065018.
Ebrahimi, F. and Barati, M.R. (2018a), "Damping vibration analysis of graphene sheets on viscoelastic medium incorporating hygro-thermal effects employing nonlocal strain gradient theory", *Compos. Struct.*, **185**, 241-253.
Ebrahimi, F. and Barati, M.R. (2018b), "Vibration analysis of size-dependent flexoelectric nanoplates incorporating surface and thermal effects", *Mech. Adv. Mater. Struct.*, **25**(7), 611-621.
Ebrahimi, F. and Heidari, E. (2017), "Surface effects on nonlinear vibration of embedded functionally graded nanoplates via higher order shear deformation plate theory", *Mech. Adv. Mater. Struct.*, 1-29.
Ebrahimi, F. and Hosseini, S. (2016a), "Double nanoplate-based NEMS under hydrostatic and electrostatic actuations", *Eur. Phys. J. Plus*, **131**(5), 160.
Ebrahimi, F. and Hosseini, S. (2016b), "Thermal effects on nonlinear vibration behavior of viscoelastic nanosize plates", *J. Therm. Stress.*, **39**(5), 606-625.
Ebrahimi, F. and Salari, E. (2015), "Thermal buckling and free vibration analysis of size dependent Timoshenko FG nanobeams in thermal environments", *Compos. Struct.*, **128**, 363-380.
Ebrahimi, F. and Shafiei, N. (2017), "Influence of initial shear stress on the vibration behavior of single-layered graphene sheets embedded in an elastic medium based on Reddy's higher-order shear deformation plate theory", *Adv. Mater. Struct.*, **24**(9), 761-772.
Ebrahimi, F., Hamed, S. and Hosseini, S. (2016), "Nonlinear electroelastic vibration analysis of NEMS consisting of double-viscoelastic nanoplates", *Appl. Phys. A*, **122**(10), 922.
Ebrahimi, F., Barati, M.R. and Haghi, P. (2017), "Thermal effects on wave propagation characteristics of rotating strain gradient temperature-dependent functionally graded nanoscale beams", *J. Therm. Stress.*, **40**(5), 535-547.
Ebrahimi, F. and Barati, M.R. (2016g), "Vibration analysis of smart piezoelectrically actuated nanobeams subjected to magneto-electrical field in thermal environment", *J. Vibr. Contr.*, 1077546316646239.
Ebrahimi, F. and Barati, M.R. (2016h), "Buckling analysis of nonlocal third-order shear deformable functionally graded piezoelectric nanobeams embedded in elastic medium", *J. Brazil. Soc. Mech. Sci. Eng.*, 1-16.
Ebrahimi, F. and Barati, M.R. (2016i), "Small scale effects on hygro-thermo-mechanical vibration of temperature dependent nonhomogeneous nanoscale beams", *Mech. Adv. Mater. Struct.*, Just Accepted.
Ebrahimi, F. and Barati, M.R. (2016j), "Dynamic modeling of a thermo–piezo-electrically actuated nanosize beam subjected to a magnetic field", *Appl. Phys. A*, **122**(4), 1-18.
Ebrahimi, F. and Barati, M.R. (2016k), "Magnetic field effects on buckling behavior of smart size-dependent graded nanoscale beams", *Eur. Phys. J. Plus*, **131**(7), 1-14.
Ebrahimi, F. and Barati, M.R. (2016l), "Vibration analysis of nonlocal beams made of functionally graded material in thermal environment", *Eur. Phys. J. Plus*, **131**(8), 279.
Ebrahimi, F. and Barati, M.R. (2016m), "A nonlocal higher-order refined magneto-electro-viscoelastic beam model for dynamic analysis of smart nanostructures", *Int. J. Eng. Sci.*, **107**, 183-196.
Ebrahimi, F. and Barati, M.R. (2016n), "Small-scale effects on hygro-thermo-mechanical vibration of temperature-dependent nonhomogeneous nanoscale beams", *Mech. Adv. Mater. Struct.*, 1-13.
Ebrahimi, F. and Barati, M.R. (2016o), "A unified formulation for dynamic analysis of nonlocal heterogeneous nanobeams in hygro-thermal environment", *Appl. Phys. A*, **122**(9), 792.
Ebrahimi, F. and Barati, M.R. (2016p), "Electromechanical buckling behavior of smart piezoelectrically actuated higher-order size-dependent graded nanoscale beams in thermal environment", *Int. J. Smart Nano Mater.*, **7**(2), 69-90.
Ebrahimi, F. and Barati, M.R. (2016q), "Wave propagation analysis of quasi-3D FG nanobeams in thermal environment based on nonlocal strain gradient theory", *Appl. Phys. A*, **122**(9), 843.
Ebrahimi, F. and Barati, M.R. (2016r), "Flexural wave propagation analysis of embedded S-FGM nanobeams under longitudinal magnetic field based on nonlocal strain gradient theory", *Arab. J. Sci. Eng.*, 1-12.
Ebrahimi, F. and Barati, M.R. (2016s), "On nonlocal characteristics of curved inhomogeneous Euler-Bernoulli nanobeams under different temperature distributions", *Appl. Phys. A*, **122**(10), 880.
Ebrahimi, F. and Barati, M.R. (2016t), "Buckling analysis of piezoelectrically actuated smart nanoscale plates subjected to magnetic field", *J. Intellig. Mater. Syst. Struct.*, 1045389X16672569.
Ebrahimi, F. and Barati, M.R. (2016u), "Size-dependent thermal stability analysis of graded piezomagnetic nanoplates on elastic medium subjected to various thermal environments", *Appl. Phys. A*, **122**(10), 910.
Ebrahimi, F. and Barati, M.R. (2016v), "Magnetic field effects on dynamic behavior of inhomogeneous thermo-piezo-electrically actuated nanoplates", *J. Brazil. Soc. Mech. Sci. Eng.*, 1-21.
Ebrahimi, F. and Barati, M.R. (2017a), "Hygrothermal effects on vibration characteristics of viscoelastic FG nanobeams based on nonlocal strain gradient theory", *Compos. Struct.*, **159**, 433-444.
Ebrahimi, F. and Barati, M.R. (2017b), "A nonlocal strain gradient refined beam model for buckling analysis of size-dependent shear-deformable curved FG nanobeams", *Compos. Struct.*, **159**, 174-182.
Ebrahimi, F., Ghadiri, M., Salari, E., Hoseini, S.A.H. and Shaghaghi, G.R. (2015), "Application of the differential transformation method for nonlocal vibration analysis of functionally graded nanobeams", *J. Mech. Sci. Technol.*, **29**,

1207-1215.
Ebrahimi, F., Ehyaei, J. and Babaei, R. (2016), "Thermal buckling of FGM nanoplates subjected to linear and nonlinear varying loads on Pasternak foundation", *Adv. Mater. Res.*, **5**(4), 245-261.
Ebrahimi, F. and Jafari, A. (2016), "Buckling behavior of smart MEE-FG porous plate with various boundary conditions based on refined theory", *Adv. Mater. Res.*, **5**(4), 261-276.
Ebrahimi, F. and Barati, M.R. (2016), "An exact solution for buckling analysis of embedded piezoelectro-magnetically actuated nanoscale beams", *Adv. Nano Res.*, **4**(2), 65-84.
Ebrahimi, F. and Salari, E. (2015), "Size-dependent free flexural vibrational behavior of functionally graded nanobeams using semi-analytical differential transform method", *Compos. B*, **79**, 156-169.
Ebrahimi, F. and Salari, E. (2015), "Thermal buckling and free vibration analysis of size dependent Timoshenko FG nanobeams in thermal environments", *Compos. Struct.*, **128**, 363-380.
Ebrahimi, F. and Salari, E. (2015), "Thermo-mechanical vibration analysis of nonlocal temperature-dependent FG nanobeams with various boundary conditions", *Compos. B*, **78**, 272-290.
Ebrahimi F. and Mohsen, D. (2016), "Dynamic modeling of embedded curved nanobeams incorporating surface effects", *Coupled Syst. Mech.*, **5**(3).
El-Haina, F., Bousahla, A.A., Tounsi, A. and Mahmoud, S.R. (2017), "A simple analytical approach for thermal buckling of thick functionally graded sandwich plates", *Struct. Eng. Mech.*, **63**(5), 585-595.
Eringen, A.C. (1972), "On nonlocal elasticity", *Int. J. Eng. Sci.*, **10**(3), 233-248.
Eringen, A.C. (1983), "On differential equations of nonlocal elasticity and solutions of screw dislocation and surface waves", *J. Appl. Phys.*, **54**(9), 4703-4710.
Fourn, H., Atmane, H.A., Bourada, M., Bousahla, A.A., Tounsi, A. and Mahmoud, S.R. (2018), "A novel four variable refined plate theory for wave propagation in functionally graded material plates", *Steel Compos. Struct.*, **27**(1), 109-122.
Ghassabi, A., Alipour, A., Dag, S. and Cigeroglu, E. (2017), "Free vibration analysis of functionally graded rectangular nanoplates considering spatial variation of the nonlocal parameter", *Arch. Mech.*, **69**(2).
Gürses, M., Civalek, Ö., Korkmaz, A.K. and Ersoy, H. (2009), "Free vibration analysis of symmetric laminated skew plates by discrete singular convolution technique based on first-order shear deformation theory", *Int. J. Numer. Meth. Eng.*, **79**(3), 290-313.
Gurtin, M.E. and Murdoch, A.I. (1975), "A continuum theory of elastic material surfaces", *Arch. Rat. Mech. Analy.*, **57**(4), 291-323.
Gurtin, M.E. and Murdoch, A.I. (1978), "Surface stress in solids", *Int. J. Sol. Struct.*, **14**(6), 431-440.
Hosseini, M., Jamalpoor, A. and Fath, A. (2017), "Surface effect on the biaxial buckling and free vibration of FGM nanoplate embedded in visco-Pasternak standard linear solid-type of foundation", *Meccan.*, **52**(6), 1381-1396.
Hull, R. (1999), *Properties of Crystalline Silicon*, IET.
Ibach, H. (1997), "The role of surface stress in reconstruction, epitaxial growth and stabilization of mesoscopic structures", *Surf. Sci. Rep.*, **29**(5-6), 195-263.
Javaheri, R. and Eslami, M.R. (2002), "Thermal buckling of functionally graded plates", *AIAA J.*, **40**(1), 162-169.
Jung, W.Y., Park, W.T. and Han, S.C. (2014), "Bending and vibration analysis of S-FGM microplates embedded in Pasternak elastic medium using the modified couple stress theory", *Int. J. Mech. Sci.*, **87**, 150-162.
Karimi, M., Mirdamadi, H.R. and Shahidi, A.R. (2017), "Positive and negative surface effects on the buckling and vibration of rectangular nanoplates under biaxial and shear in-plane loadings based on nonlocal elasticity theory", *J. Brazil. Soc. Mech. Sci. Eng.*, **39**(4), 1391-1404.
Kim, Y.W. (2005), "Temperature dependent vibration analysis of functionally graded rectangular plates", *J. Sound Vibr.*, **284**(3), 531-549.
Lee, W.H., Han, S.C. and Park, W.T. (2015), "A refined higher order shear and normal deformation theory for E-, P-, and S-FGM plates on Pasternak elastic foundation", *Compos. Struct.*, **122**, 330-342.
Liew, K.M., Zhang, Y. and Zhang, L.W. (2017), "Nonlocal elasticity theory for graphene modeling and simulation: Prospects and challenges", *J. Model. Mech. Mater.*, **1**(1).
Lu, P., He, L.H., Lee, H.P. and Lu, C. (2006), "Thin plate theory including surface effects", *Int. J. Sol. Struct.*, **43**(16), 4631-4647.
Malekzadeh, P. (2007), "A differential quadrature nonlinear free vibration analysis of laminated composite skew thin plates", *Thin-Wall. Struct.*, **45**(2), 237-250.
Malekzadeh, P. and Shojaee, M. (2015), "A two-variable first-order shear deformation theory coupled with surface and nonlocal effects for free vibration of nanoplates", *J. Vibr. Contr.*, **21**(14), 2755-2772.
Menasria, A., Bouhadra, A., Tounsi, A., Bousahla, A.A. and Mahmoud, S.R. (2017), "A new and simple HSDT for thermal stability analysis of FG sandwich plates", *Steel Compos. Struct.*, **25**(2), 157-175.
Mondolfo, L.F. (2013), *Aluminum Alloys: Structure and Properties*, Elsevier.
Nami, M.R. and Janghorban, M. (2015), "Free vibration of functionally graded size dependent nanoplates based on second order shear deformation theory using nonlocal elasticity theory", *Iran. J. Sci. Technol. Trans. Mech. Eng.*, **39**, 15-28.
Nguyen, N.T., Hui, D., Lee, J. and Xuan, H.N. (2015), "An efficient computational approach for size-dependent analysis of functionally graded nanoplates", *Comput. Meth. Appl. Mech. Eng.*, **297**, 191-218.
Panyatong, M., Chinnaboon, B. and Chucheepsakul, S. (2015), "Nonlocal second-order shear deformation plate theory for free vibration of nanoplates", *Suranar. J. Sci. Technol.*, **22**(4), 339-348.
Panyatong, M., Chinnaboon, B. and Chucheepsakul, S. (2016), "Free vibration analysis of FG nanoplates embedded in elastic medium based on second-order shear deformation plate theory and nonlocal elasticity", *Compos. Struct.*, **153**, 428-441.
Poirier, D.R. and Geiger, G.H. (2016), *Transport Phenomena in Materials Processing*, Springer.
Praveen, G.N. and Reddy, J.N. (1998), "Nonlinear transient thermoelastic analysis of functionally graded ceramic-metal plates", *Int. J. Sol. Struct.*, **35**(33), 4457-4476.
Qian, L.F., Batra, R.C. and Chen, L.M. (2004), "Static and dynamic deformations of thick functionally graded elastic plates by using higher-order shear and normal deformable plate theory and meshless local Petrov-Galerkin method", *Compos. Part B: Eng.*, **35**(6), 685-697.
Reddy, J.N. (1984), "A refined nonlinear theory of plates with transverse shear deformation", *Int. J. Sol. Struct.*, **20**(9), 881-896.
Reddy, J.N. (2006), *Theory and Analysis of Elastic Plates and Shells*, CRC press.
Reddy, J.N. (2010), "Nonlocal nonlinear formulations for bending of classical and shear deformation theories of beams and plates", *Int. J. Eng. Sci.*, **48**(11), 1507-1518.
Reddy, J.N. (2011), "A general nonlinear third-order theory of functionally graded plates", *Int. J. Aerosp. Lightw. Struct.*, **1**(1), 1-21.

Salehipour, H., Nahvi, H. and Shahidi, A.R. (2015), "Exact analytical solution for free vibration of functionally graded micro/nanoplates via three-dimensional nonlocal elasticity", *Phys. E: Low-Dimens. Syst. Nanostruct.*, **66**, 350-358.

Sekkal, M., Fahsi, B., Tounsi, A. and Mahmoud, S.R. (2017), "A new quasi-3D HSDT for buckling and vibration of FG plate", *Struct. Eng. Mech.*, **64**(6), 737-749.

Shaat, M., Mahmoud, F.F., Alshorbagy, A.E. and Alieldin, S.S. (2013), "Bending analysis of ultra-thin functionally graded Mindlin plates incorporating surface energy effects", *Int. J. Mech. Sci.*, **75**, 223-232.

Shen, H.S. (2016), *Functionally Graded Materials: Nonlinear Analysis of Plates and Shells*, CRC Press.

Shu, C. (2012), *Differential Quadrature and Its Application in Engineering*, Springer Science & Business Media, Singapore.

Sobhy, M. (2015), "A comprehensive study on FGM nanoplates embedded in an elastic medium", *Compos. Struct.*, **134**, 966-980.

Sobhy, M. and Radwan, A.F. (2017), "A new quasi 3D nonlocal plate theory for vibration and buckling of FGM nanoplates", *Int. J. Appl. Mech.*, **9**(1), 1750008.

Swarnakar, A.K., Biest, O.V. and Vanhellemont, J. (2014), "Determination of the Si Young's modulus between room and melt temperature using the impulse excitation technique", *Phys. Stat. Sol.*, **11**(1), 150-155.

Thai, H.T. and Kim, S.E. (2013), "A simple quasi-3D sinusoidal shear deformation theory for functionally graded plates", *Compos. Struct.*, **99**, 172-180.

Vasiliev, V.V. and Morozov, E.V. (2013), *Advanced Mechanics of Composite Materials and Structural Elements*, Newnes.

Yahia, S.A., Atmane, H.A., Houari, M.A. and Tounsi, A. (2015), "Wave propagation in functionally graded plates with porosities using various higher-order shear deformation plate theories", *Struct. Eng. Mech.*, **53**(6), 1143-1165.

Yazid, M., Heireche, H., Tounsi, A., Bousahla, A.A. and Houari, M.A. (2018), "A novel nonlocal refined plate theory for stability response of orthotropic single-layer graphene sheet resting on elastic medium", *Smart Struct. Syst.*, **21**(1), 15-25.

Youcef, D.O., Kaci, A., Benzair, A., Bousahla, A.A. and Tounsi, A. (2018), "Dynamic analysis of nanoscale beams including surface stress effects", *Smart Struct. Syst.*, **21**(1), 65-74.

Younsi, A., Tounsi, A., Zaoui, F.Z., Bousahla, A.A. and Mahmoud, S.R. (2018), "Novel quasi-3D and 2D shear deformation theories for bending and free vibration analysis of FGM plates", *Geomech. Eng.*, **14**(6), 519-532.

Zare, M., Nazemnezhad, R. and Hashemi, S.H. (2015), "Natural frequency analysis of functionally graded rectangular nanoplates with different boundary conditions via an analytical method", *Meccan.*, **50**(9), 2391-2408.

Zidi, M., Tounsi, A., Houari, M.A. and Bég, O.A. (2014), "Bending analysis of FGM plates under hygro-thermo-mechanical loading using a four variable refined plate theory", *Aerosp. Sci. Technol.*, **34**, 24-34.

CC

Appendix A: Coefficients of governing and boundary equations

$$cz1 = z - \frac{4z^3}{3h^2} \qquad cz2 = -\frac{4z^3}{3h^2} \qquad cz2^{+} = cz2|_{z=h/2}$$

$$cz2^{-} = cz2|_{z=-h/2} \qquad Ev = \frac{E}{1+v} \qquad vp = \frac{v}{1-v}$$

$$Fz = (\tau_0^{+} + \tau_0^{-})\frac{z}{h} + 0.5(\tau_0^{+} - \tau_0^{-}) \qquad Gz = (\rho_0^{+} + \rho_0^{-})\frac{z}{h} - 0.5(\rho_0^{-} - \rho_0^{+}) \qquad Aij = \int_{-h/2}^{h/2} aij\, dz$$

$$Aijz = \int_{-h/2}^{h/2} aij\, z\, dz \qquad Aijzn = \int_{-h/2}^{h/2} aij\, z^n\, dz \qquad a22 = a11 = Ev(1+vp)cz2 + vp\, Fz$$

$$a12 = Ev\, vp\, cz2 + vp\, Fz \qquad a25 = a14 = Ev(1+vp) \qquad 2\,a28 = a24 = 2\,a19 = a15 = Ev\, vp$$

$$a27 = a16 = Ev(1+vp)cz1 \qquad a26 = a17 = Ev\, vp\, cz1 \qquad a29 = a18 = 0.5\, Ev(1+vp)$$

$$a210 = a110 = -vp\, Gz \qquad a21 = Ev\, vp\, cz2 + vp\, Fz \qquad a31 = Ev\, cz2$$

$$a36 = a32 = a33 = 0.5\, Ev \qquad a34 = a35 = 0.5\, Ev\, cz1 \qquad a41 = 0.5\, Ev\,(1 + \frac{dcz2}{dz})$$

$$a51 = 0.5\, Ev\, \frac{dcz1}{dz} \qquad Bijt = Bij^{+} \qquad Bijb = Bij^{-}$$

$$B22^{\pm} = B11^{\pm} = 2\left(\mu_0^{\pm} - \tau_0^{\pm}\right)cz2^{\pm} + \left(\lambda_0^{\pm} + \tau_0^{\pm}\right)cz2^{\pm} + \tau_0^{\pm}\, cz2^{\pm} \qquad B21^{\pm} = B12^{\pm} = \left(\lambda_0^{\pm} + \tau_0^{\pm}\right)cz2^{\pm}$$

$$B25^{\pm} = B14^{\pm} = (2\mu_0^{\pm} + \lambda_0^{\pm}) \qquad B24^{\pm} = 2B28^{\pm} = 2B19^{\pm} = B15^{\pm} = (\tau_0^{\pm} + \lambda_0^{\pm}) \qquad B27^{\pm} = B16^{\pm} = 2\left(\mu_0^{\pm} - \tau_0^{\pm}\right)cz1^{\pm} + \left(\lambda_0^{\pm} + \tau_0^{\pm}\right)cz1^{\pm} + \tau_0^{\pm}\, cz1^{\pm}$$

$$B26^{\pm} = B17^{\pm} = \left(\tau_0^{\pm} + \lambda_0^{\pm}\right)cz1^{\pm} \qquad B29^{\pm} = B18^{\pm} = \mu_0^{\pm} + 0.5\,(\lambda_0^{\pm} - \tau_0^{\pm}) \qquad B42^{\pm} = B32^{\pm} = 2\left(\mu_0^{\pm} - \tau_0^{\pm}\right)cz2^{\pm} + \tau_0^{\pm}\, cz2^{\pm}$$

$$B44^{\pm} = B33^{\pm} = \mu_0^{\pm} \qquad B47^{\pm} = B43^{\pm} = B37^{\pm} = B34^{\pm} = \mu_0^{\pm} - \tau_0^{\pm} \qquad B46^{\pm} = B35^{\pm} = \left(\mu_0^{\pm} - \tau_0^{\pm}\right)cz1^{\pm} + \tau_0^{\pm}\, cz1^{\pm}$$

$$B45^{\pm} = B36^{\pm} = \left(\mu_0^{\pm} - \tau_0^{\pm}\right)cz1^{\pm} \qquad D11 = \frac{(-B11t - B11b - A11)h}{a^3 E_c}$$

$$D12 = \frac{\left(-B12t - B12b - A12 - A31 - \frac{B32t}{2} - \frac{B42t}{2} - \frac{B32b}{2} - \frac{B42b}{2}\right)h}{a\, E_c b^2} \qquad D14 = \frac{-B16t - B16b - A16}{a^2 E_c}$$

$$D15 = \frac{-A34 - \frac{B35t}{2} - \frac{B45t}{2} - \frac{B35b}{2} - \frac{B45b}{2}}{b^2 E_c} \qquad D16 = \frac{-B17t - B17b - A17 - A35 - \left(\frac{1}{2}\right)B36t - \left(\frac{1}{2}\right)B46t - \left(\frac{1}{2}\right)B36b - \left(\frac{1}{2}\right)B46b}{b\, a\, EN}$$

$$D17 = \frac{-B14t - B14b - A14}{a\, EN} \qquad D18 = \frac{\left(-A32 - \left(\frac{1}{2}\right)B33t - \left(\frac{1}{2}\right)B43t - \left(\frac{1}{2}\right)B33b - \left(\frac{1}{2}\right)B43b\right)a}{b^2 EN}$$

$$D19 = \frac{-B15t - B15b - A15 - A33 - \left(\frac{1}{2}\right)B34t - \left(\frac{1}{2}\right)B44t - \left(\frac{1}{2}\right)B34b - \left(\frac{1}{2}\right)B44b}{a\, EN}$$

$$D111 = \frac{(-2\,A18 - 2\,B18b - 2\,B18t)h^2}{a^3 EN} \qquad D112 = \frac{\left(-2\,A19 - 2\,B19t - 2\,B19b - \left(\frac{1}{2}\right)B47b - \left(\frac{1}{2}\right)B47t - \left(\frac{1}{2}\right)B37t - A36 - \left(\frac{1}{2}\right)B37b\right)h^2}{b^2 a\, EN}$$

$$D113 = \frac{\left(-A36 - \left(\frac{1}{2}\right)B37t - \left(\frac{1}{2}\right)B47b - \left(\frac{1}{2}\right)B37b - \left(\frac{1}{2}\right)B47t\right)h^2}{a\, b^2 EN} \qquad F12 = \bar{\mu}\frac{I_0 h^2}{a^3 \rho_c}$$

$$F11 = \frac{\left(A110 + \frac{\left(\frac{4}{3}\right)I_3}{h^2}\right)h}{a^3 \rho_c} \qquad F13 = \bar{\mu}\frac{I_0 h^2}{b^2 a\, \rho_c} \qquad F14 = -\frac{I_0}{a\, \rho_c}$$

$$F15 = -\frac{I13}{\rho_c\, a^2} \qquad F16 = -\left(\frac{4}{3}\right)I_3 \bar{\mu}\frac{h}{a^5 \rho_c} \qquad F17 = -\left(\frac{4}{3}\right)I_3 \bar{\mu}\frac{h}{b^2 a^3 \rho_c}$$

$$F18 = I13\,\bar{\mu}\frac{h^2}{a^4 \rho_c} \qquad F19 = I13\,\bar{\mu}\frac{h^2}{b^2 \rho_c\, a^2} \qquad D21 = \frac{(-A22 - B22t - B22b)h}{b^3 E_c}$$

$$D22 = \frac{\left(-\left(\frac{1}{2}\right)B42t - \left(\frac{1}{2}\right)B32b - \left(\frac{1}{2}\right)B42b - A21 - B21t - B21b - A31 - \left(\frac{1}{2}\right)B32t\right)h}{b\, a^2 E_c}$$

$$D24 = \frac{-\left(\frac{1}{2}\right)B45t - \left(\frac{1}{2}\right)B35b - \left(\frac{1}{2}\right)B45b - A26 - B26t - B26b - A34 - \left(\frac{1}{2}\right)B35t}{b\, a\, E_c} \qquad D25 = \frac{-\left(\frac{1}{2}\right)B36t - \left(\frac{1}{2}\right)B46t - \left(\frac{1}{2}\right)B36b - \left(\frac{1}{2}\right)B46b - A35}{a^2 E_c}$$

$$D27 = \frac{-\left(\frac{1}{2}\right)B43t - \left(\frac{1}{2}\right)B33b - \left(\frac{1}{2}\right)B43b - A24 - B24t - B24b - A32 - \left(\frac{1}{2}\right)B33t}{b\, E_c} \qquad D26 = \frac{-A27 - B27t - B27b}{b^2 E_c}$$

$$D28 = \frac{\left(-\left(\frac{1}{2}\right)B44t - \left(\frac{1}{2}\right)B34b - \left(\frac{1}{2}\right)B44b - A33 - \left(\frac{1}{2}\right)B34t\right)b}{a^2 E_c} \qquad D210 = \frac{-A25 - B25t - B25b}{b\ E_c}$$

$$D211 = \frac{\left(-A36 - \left(\frac{1}{2}\right)B37t - \left(\frac{1}{2}\right)B47b - \left(\frac{1}{2}\right)B37b - \left(\frac{1}{2}\right)B47t\right)h^2}{b\, a^2\, E_c}$$

Appendix B: Coefficients of governing and boundary equations

$$D212 = \frac{\left(-A36 - \left(\frac{1}{2}\right)B47t - \left(\frac{1}{2}\right)B37t - \left(\frac{1}{2}\right)B37b - 2\,B28b - 2\,B28t - 2\,A28 - \left(\frac{1}{2}\right)B47b\right)h^2}{a^2 b\ E_c}$$

$$D213 = \frac{(-2\,A29 - 2\,B29b - 2\,B29t)h^2}{b^3\ E_c}$$

$$F21 = \bar{\mu}\frac{I_0 h^2 b}{a^4\ \rho_c}$$

$$F22 = \bar{\mu}\frac{I_0 h^2}{b\ \rho_c a^2}$$

$$F23 = \frac{\left(\frac{\left(\frac{4}{3}\right)I_3}{h^2} + A210\right)h}{b\ \rho_c a^2}$$

$$F24 = -\frac{I_0 b}{\rho_c a^2}$$

$$F25 = -\left(\frac{4}{3}\right)I_3\,\bar{\mu}\frac{h}{b^3\ \rho_c a^2}$$

$$F26 = -\left(\frac{4}{3}\right)I_3\,\bar{\mu}\frac{h}{b\,a^4\,\rho_c}$$

$$F27 = I_{13}\,\bar{\mu}\frac{h^2}{a^4\ \rho_c}$$

$$F28 = I_{13}\,\bar{\mu}\frac{h^2}{b^2\ \rho_c a^2}$$

$$F29 = -\frac{I_{13}}{\rho_c a^2}$$

$$D31 = \frac{\left(-A11z + \left(\frac{1}{3}\right)h\,B11b - \left(\frac{1}{3}\right)h\,B11t + \frac{\left(\frac{4}{3}\right)A11z3}{h^2}\right)h}{a^4 E_c}$$

$$D32 = \frac{\left(-A12z + \frac{\left(\frac{4}{3}\right)A31z3}{h^2} + \left(\frac{1}{6}\right)h\,B32b - \left(\frac{1}{6}\right)h\,B32t + \left(\frac{1}{6}\right)h\,B42b - \left(\frac{1}{6}\right)h\,B42t - A31z + \left(\frac{1}{3}\right)h\,B12b - \left(\frac{1}{3}\right)h\,B12t + \frac{\left(\frac{4}{3}\right)A12z3}{h^2}\right)h}{b^2 a^2 E_c}$$

$$D35 = \frac{\left(A41 - 4\frac{A41z2}{h^2}\right)h}{a^2 E_c}$$

$$D36 = \frac{-A16z + \left(\frac{1}{3}\right)h\,B16b - \left(\frac{1}{3}\right)h\,B16t + \frac{\left(\frac{4}{3}\right)A16z3}{h^2}}{a^3 E_c}$$

$$D37 = \frac{\frac{\left(\frac{4}{3}\right)A34z3}{h^2} + \left(\frac{1}{6}\right)h\,B35b - \left(\frac{1}{6}\right)h\,B35t + \left(\frac{1}{6}\right)h\,B45b - \left(\frac{1}{6}\right)h\,B45t - A34z}{b^2 E_c\ a}$$

$$D38 = \frac{A51 - 4\frac{A51z2}{h^2}}{E_c\ a}$$

$$D39 = \frac{-A17z + \frac{\left(\frac{4}{3}\right)A35z3}{h^2} + \left(\frac{1}{6}\right)h\,B36b - \left(\frac{1}{6}\right)h\,B36t + \left(\frac{1}{6}\right)h\,B46b - \left(\frac{1}{6}\right)h\,B46t - A35z + \left(\frac{1}{3}\right)h\,B17b - \left(\frac{1}{3}\right)h\,B17t + \frac{\left(\frac{4}{3}\right)A17z3}{h^2}}{b\ a^2 E_c}$$

$$D311 = \frac{-A14z + \left(\frac{1}{3}\right)h\,B14b - \left(\frac{1}{3}\right)h\,B14t + \frac{\left(\frac{4}{3}\right)A14z3}{h^2}}{a^2 E_c}$$

$$D312 = \frac{\frac{\left(\frac{4}{3}\right)A32z3}{h^2} + \left(\frac{1}{6}\right)h\,B33b - \left(\frac{1}{6}\right)h\,B33t + \left(\frac{1}{6}\right)h\,B43b - \left(\frac{1}{6}\right)h\,B43t - A32z}{b^2 E_c}$$

$$D313 = \frac{-A15z + \frac{\left(\frac{4}{3}\right)A33z3}{h^2} + \left(\frac{1}{6}\right)h\,B34b - \left(\frac{1}{6}\right)h\,B34t + \left(\frac{1}{6}\right)h\,B44b - \left(\frac{1}{6}\right)h\,B44t - A33z + \left(\frac{1}{3}\right)h\,B15b - \left(\frac{1}{3}\right)h\,B15t + \frac{\left(\frac{4}{3}\right)A15z3}{h^2}}{a^2 E_c}$$

$$D314 = \frac{\left(-2\,A18z + \left(\frac{2}{3}\right)h\,B18b - \left(\frac{2}{3}\right)h\,B18t + \frac{\left(\frac{8}{3}\right)A18z3}{h^2}\right)h^2}{a^4 E_c}$$

$$D315 = \frac{\left(\frac{\left(\frac{4}{3}\right)A36z3}{h^2} + \left(\frac{1}{6}\right)h\,B37b - \left(\frac{1}{6}\right)h\,B37t + \left(\frac{1}{6}\right)h\,B47b - \left(\frac{1}{6}\right)h\,B47t - 2\,A19z - A36z + \left(\frac{2}{3}\right)h\,B19b - \left(\frac{2}{3}\right)h\,B19t + \frac{\left(\frac{8}{3}\right)A19z3}{h^2}\right)h^2}{b^2 a^2 E_c}$$

$$D316 = \frac{\left(\frac{\left(\frac{4}{3}\right)A36z3}{h^2} + \left(\frac{1}{6}\right)h\,B37b - \left(\frac{1}{6}\right)h\,B37t + \left(\frac{1}{6}\right)h\,B47b - \left(\frac{1}{6}\right)h\,B47t - A36z\right)h^2}{a^2 b^2\ E_c}$$

$$F31 = -I_{246}\bar{\mu}\frac{h^2}{a^5\ \rho_c}$$

$$F32 = -I_{246}\,\bar{\mu}\frac{h^2}{b^2\ \rho_c\ a^3}$$

$$F33 = \frac{\left(-\left(\frac{4}{3}\right)\bar{\mu}\,I_4 + \left(\frac{16}{9}\right)\bar{\mu}\frac{I_6}{h^2}\right)h}{a^6\rho_c}$$

$$F34 = \frac{\left(-\left(\frac{4}{3}\right)\bar{\mu}\,I_4 + \left(\frac{16}{9}\right)\bar{\mu}\frac{I_6}{h^2}\right)h}{b^2 a^4 \rho_c}$$

$$F35 = \frac{\left(-\frac{\left(\frac{4}{3}\right)A110z3}{h^2} + \frac{\left(\frac{4}{3}\right)I_4}{h^2} - \frac{\left(\frac{16}{9}\right)I_6}{h^4} + A110z\right)h}{a^4\rho_c}$$

$$F36 = \frac{I_{246}}{\rho_c a^3}$$

$$F37 = I_{13}\frac{\bar{\mu}h^2}{a^4\ \rho_c}$$

$$F38 = I_{13}\bar{\mu}\frac{h^2}{b^2 a^2 \rho_c}$$

$$F39 = (-I_{13}a)\left(\frac{1}{\rho_c a^3}\right)$$

$$D41 = \frac{\left(\frac{\left(\frac{4}{3}\right)A22z3}{h^2} + \left(\frac{1}{3}\right)h\,B22b - \left(\frac{1}{3}\right)h\,B22t - A22z\right)h}{b^3 E_c a}$$

Appendix C: Coefficients of governing and boundary equations

$$D42 = \frac{\left(\frac{\left(\frac{4}{3}\right)A21z3}{h^2} + \left(\frac{1}{3}\right)h\,B21b - \left(\frac{1}{3}\right)h\,B21t + \frac{\left(\frac{4}{3}\right)A31z3}{h^2} + \left(\frac{1}{6}\right)h\,B32b - \left(\frac{1}{6}\right)h\,B32t + \left(\frac{1}{6}\right)h\,B42b - \left(\frac{1}{6}\right)h\,B42t - A21z - A31z\right)h}{b\,a^3E_c}$$

$$D45 = \frac{\left(A41 - 4\frac{A41z2}{h^2}\right)h}{b\,E_c a}$$

$$D46 = \frac{\frac{\left(\frac{4}{3}\right)A26z3}{h^2} + \left(\frac{1}{3}\right)h\,B26b - \left(\frac{1}{3}\right)h\,B26t + \frac{\left(\frac{4}{3}\right)A34z3}{h^2} + \left(\frac{1}{6}\right)h\,B35b - \left(\frac{1}{6}\right)h\,B35t + \left(\frac{1}{6}\right)h\,B45b - \left(\frac{1}{6}\right)h\,B45t - A26z - A34z}{b\,a^2E_c}$$

$$D47 = \frac{\frac{\left(\frac{4}{3}\right)A35z3}{h^2} + \left(\frac{1}{6}\right)h\,B36b - \left(\frac{1}{6}\right)h\,B36t + \left(\frac{1}{6}\right)h\,B46b - \left(\frac{1}{6}\right)h\,B46t - A35z}{a^3E_c}$$

$$D49 = \frac{A51 - 4\frac{A51z2}{h^2}}{E_c a}$$

$$D410 = \frac{\frac{\left(\frac{4}{3}\right)A27z3}{h^2} + \left(\frac{1}{3}\right)h\,B27b - \left(\frac{1}{3}\right)h\,B27t - A27z}{b^2E_c a}$$

$$D411 = \frac{\frac{\left(\frac{4}{3}\right)A24z3}{h^2} + \left(\frac{1}{3}\right)h\,B24b - \left(\frac{1}{3}\right)h\,B24t + \frac{\left(\frac{4}{3}\right)A32z3}{h^2} + \left(\frac{1}{6}\right)h\,B33b - \left(\frac{1}{6}\right)h\,B33t + \left(\frac{1}{6}\right)h\,B43b - \left(\frac{1}{6}\right)h\,B43t - A24z - A32z}{b\,E_c a}$$

$$D412 = \frac{\left(\frac{\left(\frac{4}{3}\right)A33z3}{h^2} + \left(\frac{1}{6}\right)h\,B34b - \left(\frac{1}{6}\right)h\,B34t + \left(\frac{1}{6}\right)h\,B44b - \left(\frac{1}{6}\right)h\,B44t - A33z\right)b}{a^3E_c}$$

$$D413 = \frac{\frac{\left(\frac{4}{3}\right)A25z3}{h^2} + \left(\frac{1}{3}\right)h\,B25b - \left(\frac{1}{3}\right)h\,B25t - A25z}{b\,E_c a}$$

$$D414 = \frac{\left(\frac{\left(\frac{4}{3}\right)A36z3}{h^2} + \left(\frac{1}{6}\right)h\,B37b - \left(\frac{1}{6}\right)h\,B37t + \left(\frac{1}{6}\right)h\,B47b - \left(\frac{1}{6}\right)h\,B47t - A36z\right)h^2}{b\,a^3E_c}$$

$$D415 = \frac{\left(\frac{\left(\frac{8}{3}\right)A28z3}{h^2} + \left(\frac{2}{3}\right)h\,B28b - \left(\frac{2}{3}\right)h\,B28t + \frac{\left(\frac{4}{3}\right)A36z3}{h^2} + \left(\frac{1}{6}\right)h\,B37b - \left(\frac{1}{6}\right)h\,B37t + \left(\frac{1}{6}\right)h\,B47b - \left(\frac{1}{6}\right)h\,B47t - A36z - 2\,A28z\right)h^2}{a^3b\,E_c}$$

$$D416 = \frac{\left(-2\,A29z + \left(\frac{2}{3}\right)h\,B29b - \left(\frac{2}{3}\right)h\,B29t + \frac{\left(\frac{8}{3}\right)A29z3}{h^2}\right)h^2}{b^3E_c a}$$

$$F41 = -I_{246}\,\bar{\mu}\frac{h^2}{a^5\rho_c}$$

$$F42 = -I_{246}\,\bar{\mu}\frac{h^2}{b^2\rho_c a^3}$$

$$F43 = \frac{\left(-\left(\frac{4}{3}\right)\bar{\mu}\,I_4 + \left(\frac{16}{9}\right)\bar{\mu}\frac{I_6}{h^2}\right)h}{b\,a^5\rho_c}$$

$$F44 = \frac{\left(-\left(\frac{4}{3}\right)\bar{\mu}\,I_4 + \left(\frac{16}{9}\right)\bar{\mu}\frac{I_6}{h^2}\right)h}{b^3\rho_c a^3}$$

$$F45 = \frac{\left(-\frac{\left(\frac{4}{3}\right)A210z3}{h^2} + \frac{\left(\frac{4}{3}\right)I_4}{h^2} - \frac{\left(\frac{16}{9}\right)I_6}{h^4} + A210z\right)h}{b\,\rho_c a^3}$$

$$F46 = \frac{I_{246}}{\rho_c a^3}$$

$$F47 = I_{13}\bar{\mu}\frac{h^2 b}{a^5\rho_c}$$

$$F48 = I_{13}\bar{\mu}\frac{h^2}{b\,\rho_c a^3}$$

$$F49 = -\frac{I_{13}b}{\rho_c a^3}$$

$$D51 = \frac{\left(-\mu\,h^2K_p - \frac{\left(\frac{4}{3}\right)A11z3}{h^2} + \left(\frac{1}{6}\right)h\,B11b - \left(\frac{1}{6}\right)h\,B11t\right)h}{a^4E_c}$$

$$D52 = \frac{\left(-\mu\,h^2K_p - \frac{\left(\frac{4}{3}\right)A22z3}{h^2} - \left(\frac{1}{6}\right)h\,B22t + \left(\frac{1}{6}\right)h\,B22b\right)h}{b^4E_c}$$

$$D547 = -\frac{K_w h}{E_c}$$

$$D54 = \frac{\left(-\frac{\left(\frac{8}{3}\right)A31z3}{h^2} - \frac{\left(\frac{4}{3}\right)A12z3}{h^2} - \frac{\left(\frac{4}{3}\right)A21z3}{h^2} + \left(\frac{1}{6}\right)h\,B21b - \left(\frac{1}{6}\right)h\,B21t + \left(\frac{1}{6}\right)h\,B12b - \left(\frac{1}{6}\right)h\,B12t + \left(\frac{1}{6}\right)h\,B32b - \left(\frac{1}{6}\right)h\,B32t + \left(\frac{1}{6}\right)h\,B42b - \left(\frac{1}{6}\right)h\,B42t - 2\,\mu\,h^2K_p\right)h}{b^2a^2E_c}$$

$$D57 = \frac{\left(K_p + 4\frac{A41z2}{h^2} + \mu\,h^2K_w - tau_{0b} - A41 - tau_{0t} + N_{xx}^T + N_{xx}^C\right)h}{a^2E_c}$$

$$D58 = h\frac{K_p + N_{yy}^C + N_{yy}^T + 4\frac{A41z2}{h^2} + h^2\mu K_w - tau_{0b} - A41 - tau_{0t}}{E_c b^2}$$

$$D59 = \frac{-\frac{\left(\frac{4}{3}\right)A16z3}{h^2} + \left(\frac{1}{6}\right)h\,B16b - \left(\frac{1}{6}\right)h\,B16t}{a^3E_c}$$

$$D510 = \frac{\left(\frac{1}{6}\right)h\,B26b - \frac{\left(\frac{8}{3}\right)A34z3}{h^2} - \left(\frac{1}{6}\right)h\,B45t - \left(\frac{1}{6}\right)h\,B26t - \frac{\left(\frac{4}{3}\right)A26z3}{h^2} - \left(\frac{1}{6}\right)h\,B35t + \left(\frac{1}{6}\right)h\,B45b + \left(\frac{1}{6}\right)h\,B35b}{b^2a\,E_c}$$

$$D511 = -\frac{A51}{a\,E_c} + 4\frac{A51z2}{a\,h^2E_c}$$

$$D512 = \frac{-\left(\frac{1}{6}\right)h\,B27t - \frac{\left(\frac{4}{3}\right)A27z3}{h^2} + \left(\frac{1}{6}\right)h\,B27b}{b^3E_c}$$

Appendix D: Coefficients of governing and boundary equations

$$D513 = \frac{\left(\frac{1}{6}\right)h\,B17b - \left(\frac{1}{6}\right)h\,B17t - \frac{\left(\frac{4}{3}\right)A17z3}{h^2} - \frac{\left(\frac{8}{3}\right)A35z3}{h^2} + \left(\frac{1}{6}\right)h\,B36b - \left(\frac{1}{6}\right)h\,B36t + \left(\frac{1}{6}\right)h\,B46b - \left(\frac{1}{6}\right)h\,B46t}{b\,a^2E_c}$$

$$D515 = \frac{-\frac{A51}{b} + 4\frac{A51z2}{b\,h^2}}{E_c} \qquad D516 = \frac{-\frac{\left(\frac{4}{3}\right)A14z3}{h^2} + \left(\frac{1}{6}\right)h\,B14b - \left(\frac{1}{6}\right)h\,B14t}{a^2E_c}$$

$$D517 = \frac{-\frac{\left(\frac{4}{3}\right)A24z3}{h^2} - \frac{\left(\frac{8}{3}\right)A32z3}{h^2} + \left(\frac{1}{6}\right)h\,B33b - \left(\frac{1}{6}\right)h\,B33t + \left(\frac{1}{6}\right)h\,B43b - \left(\frac{1}{6}\right)h\,B43t + \left(\frac{1}{6}\right)h\,B24b - \left(\frac{1}{6}\right)h\,B24t}{b^2E_c}$$

$$D518 = \frac{\left(\frac{1}{6}\right)h\,B25b - \left(\frac{1}{6}\right)h\,B25t - \frac{\left(\frac{4}{3}\right)A25z3}{h^2}}{b^2E_c} \qquad D519 = \frac{-\frac{\left(\frac{4}{3}\right)A15z3}{h^2} - \frac{\left(\frac{8}{3}\right)A33z3}{h^2} + \left(\frac{1}{6}\right)h\,B34b - \left(\frac{1}{6}\right)h\,B34t + \left(\frac{1}{6}\right)h\,B44b - \left(\frac{1}{6}\right)h\,B44t + \left(\frac{1}{6}\right)h\,B15b - \left(\frac{1}{6}\right)h\,B15t}{a^2E_c}$$

$$D520 = \frac{\left(-A11 - B11b - B11t - \frac{\left(\frac{8}{3}\right)A18z3}{h^2} + \left(\frac{1}{3}\right)h\,B18b - \left(\frac{1}{3}\right)h\,B18t\right)h^2}{E_c a^4}$$

$$D521 = (-2\,A31 - B32t - B42t - B32b - B42b - \tfrac{\left(\frac{8}{3}\right)A19z3}{h^2} - \tfrac{\left(\frac{8}{3}\right)A36z3}{h^2} - \tfrac{\left(\frac{8}{3}\right)A28z3}{h^2} + \left(\tfrac{1}{6}\right)h\,B37b - \left(\tfrac{1}{6}\right)h\,B37t + \left(\tfrac{1}{6}\right)h\,B47b - \left(\tfrac{1}{6}\right)h\,B47t - \left(\tfrac{1}{6}\right)h\,B47t + \left(\tfrac{1}{3}\right)h\,B28b - -\left(\tfrac{1}{3}\right)h\,B28t + \left(\tfrac{1}{3}\right)h\,B19b - \left(\tfrac{1}{3}\right)h\,B19t)h^2/E_c b^2 a^2$$

$$D522 = \frac{\left(-A22 - B22b - B22t - \frac{\left(\frac{8}{3}\right)A29z3}{h^2} + \left(\frac{1}{3}\right)h\,B29b - \left(\frac{1}{3}\right)h\,B29t\right)h^2}{E_c b^4} \qquad D523 = \frac{\left(-\frac{\left(\frac{8}{3}\right)A18z3}{h^2} + \left(\frac{1}{3}\right)h\,B18b - \left(\frac{1}{3}\right)h\,B18t\right)h^2}{E_c a^4}$$

$$D525 = \frac{\left(-A12 - B12b - B12t - A21 - B21b - B21t - \frac{\left(\frac{8}{3}\right)A36z3}{h^2} + \left(\frac{1}{6}\right)h\,B37b - \left(\frac{1}{6}\right)h\,B37t + \left(\frac{1}{6}\right)h\,B47b - \left(\frac{1}{6}\right)h\,B47t\right)h^2}{b^2a^2E_c}$$

$$D526 = \frac{\left(-\frac{\left(\frac{8}{3}\right)A29z3}{h^2} + \left(\frac{1}{3}\right)h\,B29b - \left(\frac{1}{3}\right)h\,B29t\right)h^2}{E_c b^4}$$

$$D528 = \frac{\left(-\frac{\left(\frac{8}{3}\right)A19z3}{h^2} - \frac{\left(\frac{8}{3}\right)A36z3}{h^2} + \left(\frac{1}{6}\right)h\,B37b - \left(\frac{1}{6}\right)h\,B37t + \left(\frac{1}{6}\right)h\,B47b - \left(\frac{1}{6}\right)h\,B47t + \left(\frac{1}{3}\right)h\,B19b - \left(\frac{1}{3}\right)h\,B19t\right)h^2}{E_c b^2 a^2}$$

$$D529 = \frac{\left(-\frac{\left(\frac{8}{3}\right)A28z3}{h^2} - \frac{\left(\frac{8}{3}\right)A36z3}{h^2} + \left(\frac{1}{6}\right)h\,B37b - \left(\frac{1}{6}\right)h\,B37t + \left(\frac{1}{6}\right)h\,B47b - \left(\frac{1}{6}\right)h\,B47t + \left(\frac{1}{3}\right)h\,B28b - \left(\frac{1}{3}\right)h\,B28t\right)h^2}{E_c a^2 b^2}$$

$$D530 = \frac{(-B14t - B14b - A14)h}{a^2E_c} \qquad D531 = \frac{(-A24 - B24b - B24t)h}{b^2E_c} \qquad D532 = \frac{(-2\,A32 - B33t - B43t - B33b - B43b)h}{b^2E_c}$$

$$D533 = \frac{(-2\,A33 - B34t - B44t - B34b - B44b)h}{a^2E_c} \qquad D534 = \frac{(-A15 - B15b - B15t)h}{a^2E_c}$$

$$D535 = \frac{(-A25 - B25t - B25b)h}{b^2E_c} \qquad D536 = \frac{(-A26 - B26t - B26b)h}{b^2a\,E_c} \qquad D537 = \frac{(-B16t - B16b - A16)h}{a^3E_c}$$

$$D538 = \frac{(-2\,A34 - B35t - B45t - B35b - B45b)h}{b^2a\,E_c} \qquad D539 = \frac{(-A17 - B17b - B17t)h}{a^2b\,E_c}$$

$$D540 = \frac{(-A27 - B27t - B27b)h}{b^3E_c} \qquad D541 = \frac{(-2\,A35 - B36t - B46t - B36b - B46b)h}{b\,a^2E_c} \qquad D542 = \frac{(-2\,A36 - B37t - B47t - B37b - B47b)h^3}{a^2b^2E_c}$$

$$D543 = \frac{(-A18 - B18b - B18t)h^3}{a^4E_c} \qquad D544 = \frac{(-A19 - B19b - B19t)h^3}{b^2a^2E_c} \qquad D545 = \frac{(-A29 - B29b - B29t)h^3}{b^4E_c}$$

Appendix E: Coefficients of governing and boundary equations

$$D546 = \frac{(-A28 - B28b - B28t)h^3}{a^2b^2E_c}$$

$$F51 = -\left(\frac{16}{9}\right)\bar{\mu}\frac{I_6}{h\,a^6\rho_c}$$

$$F52 = -\left(\frac{32}{9}\right)\bar{\mu}\frac{I_6}{h\,b^2a^4\rho_c}$$

$$F53 = -\left(\frac{16}{9}\right)\bar{\mu}\frac{I_6}{h\,b^4\rho_c a^2}$$

$$F54 = \frac{\left(\frac{16}{9}\right)I_6}{h^3a^4\rho_c} + \frac{\left(\frac{4}{3}\right)A110z3}{h\,a^4\rho_c} + \frac{h^3I_0\bar{\mu}}{a^4\rho_c}$$

$$F55 = \frac{\left(\frac{16}{9}\right)I_6}{h^3b^2\rho_c a^2} + \frac{\left(\frac{4}{3}\right)A210z3}{h\,b^2\rho_c a^2} + \frac{h^3I_0\bar{\mu}}{b^2\rho_c a^2}$$

$$F56 = -h\frac{I_0}{\rho_c a^2}$$

$$F57 = \frac{\left(\left(\frac{4}{3}\right)I_4 - \frac{\left(\frac{16}{9}\right)I_6}{h^2}\right)\bar{\mu}}{a^5\rho_c}$$

$$F58 = \frac{\left(\left(\frac{4}{3}\right)I_4 - \frac{\left(\frac{16}{9}\right)I_6}{h^2}\right)\bar{\mu}}{b^2a^3\rho_c}$$

$$F59 = \frac{\left(\left(\frac{4}{3}\right)I_4 - \frac{\left(\frac{16}{9}\right)I_6}{h^2}\right)\bar{\mu}}{b\,a^4\rho_c}$$

$$F510 = \frac{\left(\left(\frac{4}{3}\right)I_4 - \frac{\left(\frac{16}{9}\right)I_6}{h^2}\right)\bar{\mu}}{b^3\rho_c a^2}$$

$$F511 = \frac{h^2A110}{a^4\rho_c}$$

$$F512 = \frac{h^2A210}{b^2\rho_c a^2}$$

$$F513 = \frac{-\frac{\left(\frac{4}{3}\right)I_4}{h^2} + \frac{\left(\frac{16}{9}\right)I_6}{h^4}}{a^3\rho_c}$$

$$F514 = \frac{-\frac{\left(\frac{4}{3}\right)I_4}{h^2} + \frac{\left(\frac{16}{9}\right)I_6}{h^4}}{b\,\rho_c a^2}$$

$$F515 = \frac{\left(\frac{4}{3}\right)I_3\bar{\mu}}{a^4\rho_c}$$

$$F516 = \frac{\left(\frac{4}{3}\right)I_3\bar{\mu}}{b^2\rho_c a^2}$$

$$F517 = \frac{\left(\frac{4}{3}\right)I_3\bar{\mu}}{a^4\rho_c}$$

$$F518 = \frac{\left(\frac{4}{3}\right)I_3\bar{\mu}}{b^2\rho_c a^2}$$

$$F519 = -\frac{\left(\frac{4}{3}\right)I_3}{h^2\rho_c a^2}$$

$$F520 = -\frac{\left(\frac{4}{3}\right)I_3}{h^2\rho_c a^2}$$

$$V61 = \frac{\left(A11z + \left(\frac{1}{2}\right)h\,B11t - \left(\frac{1}{2}\right)h\,B11b\right)h}{a^4E_c}$$

$$V62 = \frac{\left(A12z + \left(\frac{1}{2}\right)h\,B12t - \left(\frac{1}{2}\right)h\,B12b\right)h}{b^2E_c a^2}$$

$$V63 = \frac{A16z + \left(\frac{1}{2}\right)h\,B16t - \left(\frac{1}{2}\right)h\,B16b}{a^3E_c}$$

$$V64 = \frac{A17z + \left(\frac{1}{2}\right)h\,B17t - \left(\frac{1}{2}\right)h\,B17b}{b\,E_c a^2}$$

$$V65 = \frac{A14z + \left(\frac{1}{2}\right)h\,B14t - \left(\frac{1}{2}\right)h\,B14b}{E_c a^2}$$

$$V66 = \frac{A15z + \left(\frac{1}{2}\right)h\,B15t - \left(\frac{1}{2}\right)h\,B15b}{E_c a^2}$$

$$V67 = \frac{\left(-\left(\frac{1}{2}\right)h\,B18b + A18z + \left(\frac{1}{2}\right)h\,B18t\right)h^2}{a^4E_c}$$

$$V68 = \frac{\left(\left(\frac{1}{2}\right)h\,B19t - \left(\frac{1}{2}\right)h\,B19b + A19z\right)h^2}{b^2E_c a^2}$$

$$V69 = \frac{\left(\frac{1}{2}\right)\tau_0^+h - \left(\frac{1}{2}\right)\tau_0^-h - M_{xx}^T - M_{xx}^C}{E_c a^2}$$

$$F61 = -A110z\frac{h}{\rho_c a^4}$$

$$V71 = \frac{(A11 + B11b + B11t)h}{a^3E_c}$$

$$V72 = \frac{(A12 + B12b + B12t)h}{b^2E_c a}$$

$$V74 = \frac{A16 + B16b + B16t}{a^2E_c}$$

$$V75 = \frac{A17 + B17b + B17t}{b\,E_c a}$$

$$V76 = \frac{A14 + B14b + B14t}{E_c a}$$

$$V77 = \frac{A15 + B15b + B15t}{E_c a}$$

$$V78 = \frac{(A18 + B18b + B18t)h^2}{a^3E_c}$$

$$V79 = \frac{(A19 + B19b + B19t)h^2}{b^2E_c a}$$

$$V710 = \frac{\tau_0^+ + \tau_0^- - N_{xx}^T - N_{xx}^C}{E_c a}$$

$$V711 = -h\frac{A110}{\rho_c a^3}$$

$$V81 = \frac{\left(A21z + \left(\frac{1}{2}\right)h\,B21t - \left(\frac{1}{2}\right)h\,B21b\right)h}{a^4E_c}$$

$$V82 = \frac{\left(A22z + \left(\frac{1}{2}\right)h\,B22t - \left(\frac{1}{2}\right)h\,B22b\right)h}{b^2E_c a^2}$$

$$V83 = \frac{A26z + \left(\frac{1}{2}\right)h\,B26t - \left(\frac{1}{2}\right)h\,B26b}{a^3E_c}$$

$$V84 = \frac{A27z + \left(\frac{1}{2}\right)h\,B27t - \left(\frac{1}{2}\right)h\,B27b}{b\,E_c a^2}$$

$$V85 = \frac{A24z + \left(\frac{1}{2}\right)h\,B24t - \left(\frac{1}{2}\right)h\,B24b}{E_c a^2}$$

$$V86 = \frac{A25z + \left(\frac{1}{2}\right)h\,B25t - \left(\frac{1}{2}\right)h\,B25b}{E_c a^2}$$

$$V87 = \frac{\left(A28z - \left(\frac{1}{2}\right)h\,B28b + \left(\frac{1}{2}\right)h\,B28t\right)h^2}{a^4E_c}$$

$$V88 = \frac{\left(A29z - \left(\frac{1}{2}\right)h\,B29b + \left(\frac{1}{2}\right)h\,B29t\right)h^2}{b^2E_c a^2}$$

$$V89 = \frac{\left(\frac{1}{2}\right)\tau_0^+h - \left(\frac{1}{2}\right)\tau_0^-h - M_{yy}^T - M_{yy}^C}{E_c a^2}$$

$$F81 = -A210z\frac{h}{\rho_c a^4}$$

$$V91 = \frac{(A21 + B21b + B21t)h}{a^3E_c}$$

$$V92 = \frac{(A22 + B22b + B22t)h}{b^2E_c a}$$

$$V94 = \frac{A26 + B26t + B26b}{a^2E_c}$$

$$V95 = \frac{A27 + B27b + B27t}{b\,E_c a}$$

$$V96 = \frac{A24 + B24b + B24t}{E_c a}$$

$$V97 = \frac{A25 + B25b + B25t}{E_c a}$$

$$V98 = \frac{(A28 + B28b + B28t)h^2}{a^3E_c}$$

$$V99 = \frac{(A29 + B29b + B29t)h^2}{b^2E_c a}$$

$$V910 = \frac{\tau_0^- + \tau_0^+ - N_{yy}^T - N_{yy}^C}{E_c a}$$

$$V911 = -h\frac{A210}{\rho_c a^3}$$

$$V101 = \frac{\left(A11z3 - \left(\frac{1}{8}\right)h^3B11b + \left(\frac{1}{8}\right)h^3B11t\right)h}{a^6E_c}$$

Appendix F: Coefficients of governing and boundary equations

$$V102 = \frac{\left(A12z3 - \left(\frac{1}{8}\right)B12b\,h^3 + \left(\frac{1}{8}\right)B12t\,h^3\right)h}{b^2E_ca^4} \qquad V104 = \frac{A16z3 - \left(\frac{1}{8}\right)h^3B16b + \left(\frac{1}{8}\right)h^3B16t}{a^5E_c} \qquad V105 = \frac{A17z3 - \left(\frac{1}{8}\right)h^3B17b + \left(\frac{1}{8}\right)B17t\,h^3}{b\,E_ca^4}$$

$$V106 = \frac{A14z3 - \left(\frac{1}{8}\right)B14b\,h^3 + \left(\frac{1}{8}\right)h^3B14t}{E_ca^4} \qquad V107 = \frac{A15z3 - \left(\frac{1}{8}\right)h^3B15b + \left(\frac{1}{8}\right)B15t\,h^3}{E_ca^4} \qquad V108 = \frac{\left(A18z3 - \left(\frac{1}{8}\right)h^3B18b + \left(\frac{1}{8}\right)h^3B18t\right)h^2}{a^6E_c}$$

$$V109 = \frac{\left(A19z3 - \left(\frac{1}{8}\right)h^3B19b + \left(\frac{1}{8}\right)h^3B19t\right)h^2}{b^2E_ca^4} \qquad V1010 = -A110z3\frac{h}{\rho_ca^6} \qquad V1011 = \frac{-\left(\frac{1}{8}\right)h^3\,\tau_0^- + \left(\frac{1}{8}\right)h^3\,\tau_0^+ - P_{xx}^T - P_{xx}^C}{E_ca^4}$$

$$V12\_1 = \frac{\left(A21z3 - \left(\frac{1}{8}\right)h^3B21b + \left(\frac{1}{8}\right)h^3B21t\right)h}{a^6E_c} \qquad V12-2 = \frac{\left(A22z3 - \left(\frac{1}{8}\right)h^3B22b + \left(\frac{1}{8}\right)h^3B22t\right)h}{b^2E_ca^4} \qquad V12-4 = \frac{A26z3 - \left(\frac{1}{8}\right)h^3B26b + \left(\frac{1}{8}\right)h^3B26t}{a^5E_c}$$

$$V12-5 = \frac{A27z3 - \left(\frac{1}{8}\right)h^3B27b + \left(\frac{1}{8}\right)h^3B27t}{b\,E_ca^4} \qquad V12-6 = \frac{A24z3 - \left(\frac{1}{8}\right)h^3B24b + \left(\frac{1}{8}\right)h^3B24t}{E_ca^4} \qquad V12-7 = \frac{A25z3 - \left(\frac{1}{8}\right)h^3B25b + \left(\frac{1}{8}\right)h^3B25t}{E_ca^4}$$

$$V12-8 = \frac{\left(A28z3 - \left(\frac{1}{8}\right)h^3B28b + \left(\frac{1}{8}\right)h^3B28t\right)h^2}{a^6E_c} \qquad V12-9 = \frac{\left(A29z3 - \left(\frac{1}{8}\right)h^3B29b + \left(\frac{1}{8}\right)h^3B29t\right)h^2}{b^2E_ca^4}$$

$$V12-10 = -A210z3\frac{h}{\rho_ca^6} \qquad V12-11 = \frac{-\left(\frac{1}{8}\right)h^3\,\tau_0^- + \left(\frac{1}{8}\right)h^3\,\tau_0^+ - P_{yy}^T - P_{yy}^C}{E_ca^4}$$